

Electroconductive Nanobiomaterials for Tissue Engineering and Regenerative Medicine

Ebrahim Mostafavi, PhD,^{1,*} David Medina-Cruz, PhD,^{1,*} Katayoon Kalantari, PhD,¹ Ada Taymoori, MD,¹ Pooneh Soltantabar, PhD,² and Thomas J. Webster, PhD¹

Abstract

Regenerative medicine aims to engineer tissue constructs that can recapitulate the functional and structural properties of native organs. Most novel regenerative therapies are based on the recreation of a three-dimensional environment that can provide essential guidance for cell organization, survival, and function, which leads to adequate tissue growth. The primary motivation in the use of conductive nanomaterials in tissue engineering has been to develop biomimetic scaffolds to recapitulate the electrical properties of the natural extracellular matrix, something often overlooked in numerous tissue engineering materials to date. In this review article, we focus on the use of electroconductive nanobiomaterials for different biomedical applications, particularly, very recent advancements for cardiovascular, neural, bone, and muscle tissue regeneration. Moreover, this review highlights how electroconductive nanobiomaterials can facilitate cell to cell crosstalk (i.e., for cell growth, migration, proliferation, and differentiation) in different tissues. Thoughts on what the field needs for future growth are also provided.

Keywords: electroconductive, tissue engineering, regenerative medicine, nanomaterials, biomaterials, nanomedicine, cardiac, bone, nerve, tendon, extracellular matrix

Introduction

Tissue engineering and regenerative medicine

ACCORDING TO STATISTICS, in the United States, one person waits for an organ transplant every 15 min.¹ Therefore, there is an unmet need for alternative approaches to fabricate artificial tissues and organs. Several factors should be taken into account when designing a system for successful organ regeneration using a tissue engineering approach, including^{2,3}: (i) resident or transplanted cells need to differentiate into specific cell types within a biomimetic matrix; (ii) the biomimetic matrix needs to provide mechanical and biological support for cell growth and function; (iii) the matrix should allow for growth factor permeation and physiological signals, such as electrical stimuli, to propagate; and (iv) the matrix should have high engraftment efficiency. Developing and testing systems that encompass all of the above have proved challenging. For example, most commonly used *in vitro* culture techniques do not mimic all of the micro and nano environmental factors that direct cell differentiation into a developing organ.

Furthermore, tissue properties such as mechanical (stiffness) and biological cues that determine cellular activity (including

cell adhesion, growth, proliferation, differentiation, and growth) should be simulated in an architected scaffold to guarantee tissue regeneration in damaged tissue.⁴ Since cellular fate is modulated by cell–scaffold interactions, efforts have been made to regulate cellular responses by controlling tissue engineering material topography, three-dimensional (3D) geometry, and/or chemical composition. Some external factors can potentially affect cell–material interactions and biocompatibility, including physical stimulation using surface topology, biochemical stimulation using the release of growth factors, and mechanical and electrical stimulation, yet all these have to be duplicated in improved artificial tissue engineering systems.

Specifically, the impact of electrical properties on tissue regeneration was originally highlighted in the 1960s when scientists showed that electrical stimulation affects bone formation,⁵ and later wound healing, nerve, myocardium, vascular endothelial cell, etc. function. Therefore, although studies have emphasized that the electrical properties of tissue engineering scaffolds should be appropriately controlled for the development of physiologically healthy artificial tissues, some polymers (such as poly-lactic-*co*-glycolic acid [PLGA]), which do not mimic natural tissue conductivity remain the gold standard in the field.

¹Department of Chemical Engineering, Northeastern University, Boston, Massachusetts, USA.

²Department of Bioengineering, University of Texas at Dallas, Richardson, Texas, USA.

*These two authors contributed equally to this work.

Over the past decade, however, some researchers have focused on biomedical applications of electroconductive nanobiomaterials; particularly, those used for biosensing, drug delivery, bioactuators, bioimaging, tissue engineering, and regenerative medicine can benefit from developments in electroactive nanobiomaterials.

The role of nanotechnology in tissue engineering and regenerative medicine

The emergence of nanotechnology has set high expectations toward meeting the complexities and difficulties in medicine and biological science. In particular, recent advances in tissue engineering and regenerative medicine, owing to nanotechnology, have revolutionized the fields of cardiovascular, neural, wound dressing, vascularization, bone, and other medicines.^{6,7}

Nanotechnology in medicine (reputed as nanomedicine) has achieved tremendous progress over the past several decades due to the close relationship between biological systems and nanoscale features. Due to the natural nanoscale features of biological systems, one can design bioassembled components and platforms using nanotechnology so it can be of great interest in life science and health care applications. Particularly, nanotechnology has opened new realms of regenerative medicine and provided novel solutions for long-term needs. Specifically, it has done so by developing desirable and ideal materials to control the chemical, biological, structural, and mechanical microenvironment for successful cell delivery and tissue regeneration. Therefore, manipulating biomaterials to create material surfaces and structures with nanoscale features (well-known as nanobiomaterials) not only can help mimic the native micro and nanoenvironment of cells, but it can also trigger select cell adhesion, growth, proliferation, and differentiation without the use of drugs.⁶

The application of nanomaterials (NMs) in medicine has led to a new field termed nanomedicine (as a bridge between nanotechnology and medicine), with great potential in the treatment of several diseases, including heart and neural diseases, bone disorders, skin and muscle disorders, etc. Therefore, NMs have become promising tools for the improved treatment and diagnosis of different disorders that are more personalized and precise than conventional methods, by eliminating many drawbacks of conventional therapies (such as adverse side-effects, not task-specific, expensive, low efficiency, and time-consuming treatment). For instance, the employment of nanoscale biomaterials (such as nanotopographies, nanoparticles, nanotubes, self-assembled materials, etc.) for tissue engineering and regenerative medicine can boost tissue regeneration while minimizing immune responses and preventing infection.

Over the past two decades, tissue engineering and regenerative medicine techniques have been regularly carried out to regenerate various tissues and organs in the body such as the heart, nerve, bone, tendon, skin, cartilage, kidney, etc. The primary objective of a 3D scaffold used for tissue regeneration is the recreation of the natural 3D environment most suitable for adequate tissue growth. An important aspect of this commitment is to mimic the fibrillar structure of the extracellular matrix (ECM), which provides essential guidance for cell organization, survival, and function. Recent advances in nanotechnology have significantly improved our capacity to mimic the ECM. Select cellular activity and intracellular signaling can be enhanced due to electrically conductive materials.^{4,8}

This review article highlights the very recent advancements in the development of different types of electroconductive nanobiomaterials (including nanofibrous scaffolds, hydrogels, hybrid scaffolds, films, and 3D printed constructs) that can recapitulate the electrical and cellular behavior of a specific tissue required for translatable regenerative medicine. Furthermore, an overview of the existing technologies and examples of these scaffolds (with particular emphasis on electroconductive scaffolds) for cardiac, nerve, bone, and skeletal muscle tissue engineering are summarized and discussed.

Electroconductive Nanobiomaterials for Biomedical Applications

Table 1 shows the range of electrical conductivity values for different native tissues extracted from *in vivo* animal models, mostly from rats. As can be seen in Table 1, to engineer different tissues in the body, researchers need to take this into account so that their engineered electroconductive nanobiomaterial scaffolds meet these electrical properties. It is noteworthy that these values are not absolute, and others can obtain values that slightly vary based on their designed measurement system and other factors.

In this review, we investigate the most recent advancements in the use of different electroconductive scaffolds at the nanoscale size for improved biomedical applications (Fig. 1).

Cardiovascular tissue engineering

Cardiovascular diseases (CVDs) are the leading cause of morbidity and mortality worldwide. The World Economic Forum estimates the total global costs from CVDs (2010–2030) are USD\$20 trillion.¹¹ CVDs can occur in different types, among which myocardial infarction (MI) captures a significant fraction of these diseases. Approximately every 40 s, an American will have a fatal MI (based on AHA computation).¹² MI is usually caused by a local obstruction of blood flow to the heart muscle, which leads to a loss of myocardial tissue and hence the formation of noncontracting scar tissue resulting in permanent impairment of the heart's pumping

TABLE 1. THE RANGE OF ELECTRICAL CONDUCTIVITY VALUES FOR DIFFERENT NATIVE TISSUES*

<i>Tissue</i>	<i>Cardiac</i>	<i>Nerve</i>	<i>Bone</i>	<i>Skeletal muscle</i>	<i>Liver</i>	<i>Lung</i>	<i>Chondrocytes</i>	<i>Endothelial cells</i>
Electrical conductivity, S/m	0.005–0.16	0.08–1.3	0.02–0.06	0.04–0.5	0.05–1	0.04–0.2	0.1–1.1	10^{-4} – 10^{-2}

*Zarrintaj et al.⁹; Stout et al.¹⁰

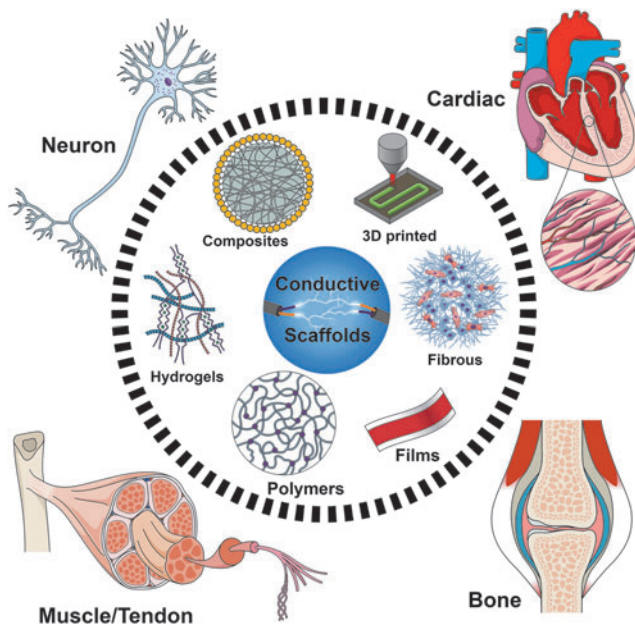


FIG. 1. Schematic illustration of different electroconductive scaffolds for biomedical applications discussed in this study.

function and if this condition is sustained over a longer time, the disease will progress and will end in chronic heart failure.¹³

Heart transplantation, while effective, is clearly limited by the availability of heart donors.¹⁴ Among other strategies to regenerate the function of an infarcted heart, the delivery of cells generally results in modest therapeutic benefits. Cell-based therapeutic approaches directed at restoring the lost myocardium through the use of adult stem cells or pluripotent stem cells have garnered interest, but they have several roadblocks, such as low viability and phenotype stability, ineffective homing of the cells, immune system rejection, exorbitant cost, etc.¹⁵

Cardiac tissue engineering holds great promise to alleviate these issues. For instance, to address some of the challenges associated with cell therapeutic approaches, embedding cells into 3D biodegradable scaffolds may better preserve cell survival and enhance cell engraftment after transplantation, consequently improving cardiac cell therapy compared with direct intramyocardial injection of isolated cells.^{16,17} Transplantation of a tissue-engineered heart (e.g., cardiac tissue patches, hydrogel, or hybrid composites functionalized with CMs) could enhance therapeutic effects by an increased engraftment rate, which in turn, results in the prolonged release of healthy cytokines, reduction in left ventricular (LV) dilation, and LV wall stresses. Another advantage of this regenerative approach is that the bioengineering of heart muscle can be achieved *ex vivo*, under precise and controllable conditions, for later implantation.

NMs for cardiovascular applications. Cardiac tissue engineering is particularly one of the fields in tissue engineering and regenerative medicine that has been revolutionized through nanostructured systems since they have solutions for both preventive and therapeutic approaches to treat CVD.¹⁴ In cardiac tissue engineering, to select the appropriate scaffold, some key parameters need to be determined, such as material

composition, surface characteristics, mechanical properties, biocompatibility, degradation rate, and cell seeding conditions. It has been discussed in some review articles^{16,18–21} that the ideal scaffold for cardiac tissue engineering would be the one that combines the following characteristics: (i) appropriate mechanical properties that match the native cardiac tissue (anisotropy, elasticity, contractility, etc.), (ii) appropriate structure that mimics the microenvironment of the native cardiac tissue (fibrous anisotropic alignment characteristic of the myocardium, porosity, nanomorphology, etc.), (iii) appropriate surface biochemistry to promote cardiac cell attachment, proliferation, viability, similar to that of the native cardiac tissue (biocompatibility, wettability, etc.), and (iv) appropriate conductivity of the scaffold to allow propagation of electrical stimulation to have a positive effect on cell behavior. Future NMs for cardiac tissue regeneration aim to provide enhanced conductivity of biomaterial scaffolds to further improve the regeneration of damaged cardiac tissue. For example, the development of nanofiber (NF) matrices as biodegradable scaffolds has provided a bottom-up approach to mimic the ECM environment. These scaffolds are able to control cell attachment, growth, and differentiation as well as promote the regeneration of various tissues.²² Therefore, NMs are increasingly becoming key components in tissue-engineered biomaterials for cardiac and vascular regeneration in patients with MI, heart failure, or coronary artery disease.

Electroconductive nanobiomaterials for cardiovascular applications. After MI, a hierarchy of irreversible events occurs in the heart leading to cell death, regional contractile dysfunction, and muscle tissue replacement by scar tissue.¹⁴ It is well known that electrical pulse signaling in the infarcted region is interdicted following the occurrence of MI, and the introduction of electrical conductivity into biomaterials has been shown to be an effective approach to promote cardiac function after MI. The development of electroconductive nanobiomaterials such as cardiac patches, hydrogels, 3D printed constructs, etc., has attracted much more attention between scientists during the past few years. These nanobiomaterials can not only simultaneously meet the biochemical, electrical, and mechanical demands of the heart tissue upon implantation, but they can also promote the regeneration of cardiomyocytes (CMs) following MI when blood stops flowing to some regions of the heart.¹¹ These nanobiomaterials can be attached to the surface of heart tissue to provide biochemical cues for regeneration and therefore provide clinically relevant *in vitro* models for cardiotoxicity assessment.

From a biomaterial perspective, the engineered cardiac tissues for treating MI are normally produced by seeding heart cells within 3D porous biomaterial scaffolds that mimic the ECM of the native tissue and organs.²³ These biomaterials, which are usually made of either biological polymers (carbohydrates, lipids, proteins, and nucleic acids), include collagen²⁴ and alginate,²³ or synthetic polymers such as poly(lactic acid) (PLA),^{8,25,26} help cells to organize into functioning tissues, but poor conductivity of these materials limits the ability of these scaffolds to contract strongly as a unit. This is mainly because of the porous properties of these engineered myocardial scaffolds, which lead to limited intercellular connection and electrical signal propagation due to isolating pore walls.^{14,27} As is well known, cardiac muscles are electrically conductive [0.005 (transverse) ~0.16

(longitudinal) S/m].¹⁰ Therefore, the proper function of engineered tissues requires mimicking the anisotropic structure of the native myocardium, which can be achieved using a series of biophysical and topographical features such as the incorporation of conductive additives, that is, carbon nanotubes (CNTs), graphene, reduced graphene oxide, gold nanomaterials (AuNMs), and conductive polymers. It is well known that the electrical pulse signal in the infarct region is interdicted following the occurrence of MI, and the introduction of conductive additives into biomaterials has been shown to be an effective approach to promote cardiac regeneration after implantation into the infarcted myocardium.²⁸

The primary motivation in the use of conductive NMs has been to develop biomimetic scaffolds to recapitulate the ECM of the native heart and to promote cardiac tissue maturity, excitability, and electrical signal propagation.²⁹ Since tissue-engineered scaffolds for cardiac regeneration are mainly made out of biopolymers that have limited synchronized capacity with the embedded cells, the conductivity of these structures can be substantially boosted by the incorporation of conductive materials/polymers into these scaffolds. Three major biomaterials that are extensively being used to improve the conductivity of bioengineered scaffolds for cardiac tissue regeneration are as follows.

Carbon-based nanobiomaterials. Presently, clinical nanomedicine and nanobiotechnology have demanded the generation of new organic/inorganic analogs of carbon-based NMs (as one of the intriguing biomedical research targets) for stem cell-based tissue engineering.³⁰ CNTs, graphene, and their chemical derivatives have been playing a pivotal role as a new class of NMs for regenerative medicine.³¹ These NMs possess excellent electrical conductivity, biocompatibility, surface area, highly favorable mechanical characteristics, rapid mass and electron transport kinetics (which are required for chemical/physical stimulation of differentiated cells), and thermal properties, and because of that they are of much interest to the scientific community. More detailed properties of these carbon-based NMs can be found in a comprehensive review article by Min et al.³² For instance, two-dimensional graphene materials have been widely used in various biomedical research areas, such as bioelectronics, imaging, drug delivery, and tissue engineering.³³ In recent years, graphene has received much interest in the design of engineered cardiac patches to regenerate a functional myocardium following infarction due to their high conductivity.²² In this regard, the success of these patches has been limited by the challenge of creating engineered tissues that can reestablish the structure and function of the native cardiac tissue across different size scales.³⁴

CNTs incorporated into scaffolds have also demonstrated a positive effect on the regeneration of cardiac tissue due to their conductivity and nanostructures. Figure 2B and C show a hydrogel-based scaffold and a hybrid-based scaffold (using a combination of nanofibrous scaffolds and a hydrogel) beneficial for cardiac cell adhesion, viability, and maturation while providing functionality for cardiac tissue applications.

Although carbon-based NMs, such as CNTs/graphene/graphene oxide (GO)-based nanocarriers, have been extensively studied due to their unique properties, the unsatisfactory biocompatibility of these NMs hampers their use in clinical settings. The physicochemical characteristics of these NMs (e.g., size, surface area, surface properties, number of layers

and particulate states) and their surface functionalization can affect its *in vitro* and *in vivo* nanotoxicity.³⁵

Gold nanomaterials. To engineer electrically conductive materials, researchers have doped different types of scaffolds with electrically conductive NMs, such as gold nanowires. In a study, Dvir et al.²³ reported the incorporation of gold nanowires (AuNWs) into an alginate-based 3D cardiac patch, and then cultured CMs onto the patches. Their results revealed that the 3D cardiac patch exhibited synchronous beating across scaffold walls and throughout the entire scaffold in the presence of nanowires, whereas CMs in pristine alginate scaffolds typically formed only small clusters that beat asynchronously and with random polarization. Their results revealed that the impedance of the scaffold biomaterial before and after modification with AuNWs was 0.5 and 12 k Ω (at 1 MHz frequency), respectively.

In another study, researchers have utilized gold nanorods (AuNRs) to develop a very different approach to introduce sutureless technology for the attachment of a cardiac patch to the injured heart. This is a promising area because although nanofibrous scaffolds as cardiac patches hold great promise for the regeneration of an infarcted heart, their integration with the infarcted myocardium might be a large problem due to the sutures used during the surgery that may cause further damage to the diseased organ. To address this issue, Malki et al.³⁶ reported the incorporation of AuNRs into albumin electrospun fibers to engineer cardiac patches for sutureless engraftment to the infarcted myocardium. After seeding the neonatal-derived CMs within the optimal scaffolds with a thickness of 60–80 μm , they positioned the functional patch on the infarcted heart followed by utilizing irradiation with a near infrared (IR) laser (808 nm, 1.5 W/cm², 120 s). The AuNRs were able to absorb IR light and convert it to energy, which provided sufficient energy for the attachment of the patch to the wall of the heart (Fig. 2A). Such a strategy can potentially be employed for the integration of any type of scaffold to the native tissue or organ while reducing the damage to the organ during the surgery as caused by conventional attachment methods, such as suturing or stitching.

However, scientists should always take the possible drawbacks of using gold nanoparticles (AuNPs) into account. For instance, researchers have shown that the physiological properties of AuNPs may change *in vivo* and thus lead to undesired and unpredicted toxicity, immune activation, or aggregation.³⁷ Therefore, although the use of conductive additives shows promising results both during *in vitro* and *in vivo* animal studies, such unexpected changes in physiological characteristics of NMs can add much more complexity to the immune system and inflammatory responses from the host body, which subsequently may lead to even more adverse effects than MI.³⁷ For instance, researchers have shown that AuNMs can be degraded in the liver or can disrupt the conformation of proteins in the body, in which both of them lead to adverse effects in the body.^{37–39}

Conductive polymeric NMs. Among conductive polymers, polyaniline (PANI), poly(3,4-ethylenedioxythiophene) (PEDOT), and polypyrrole (PPy) are the most extensively studied.⁴⁰ Detailed information about the conductivity values of these polymers, along with their other physicochemical properties, can be found elsewhere.⁴¹ One major problem

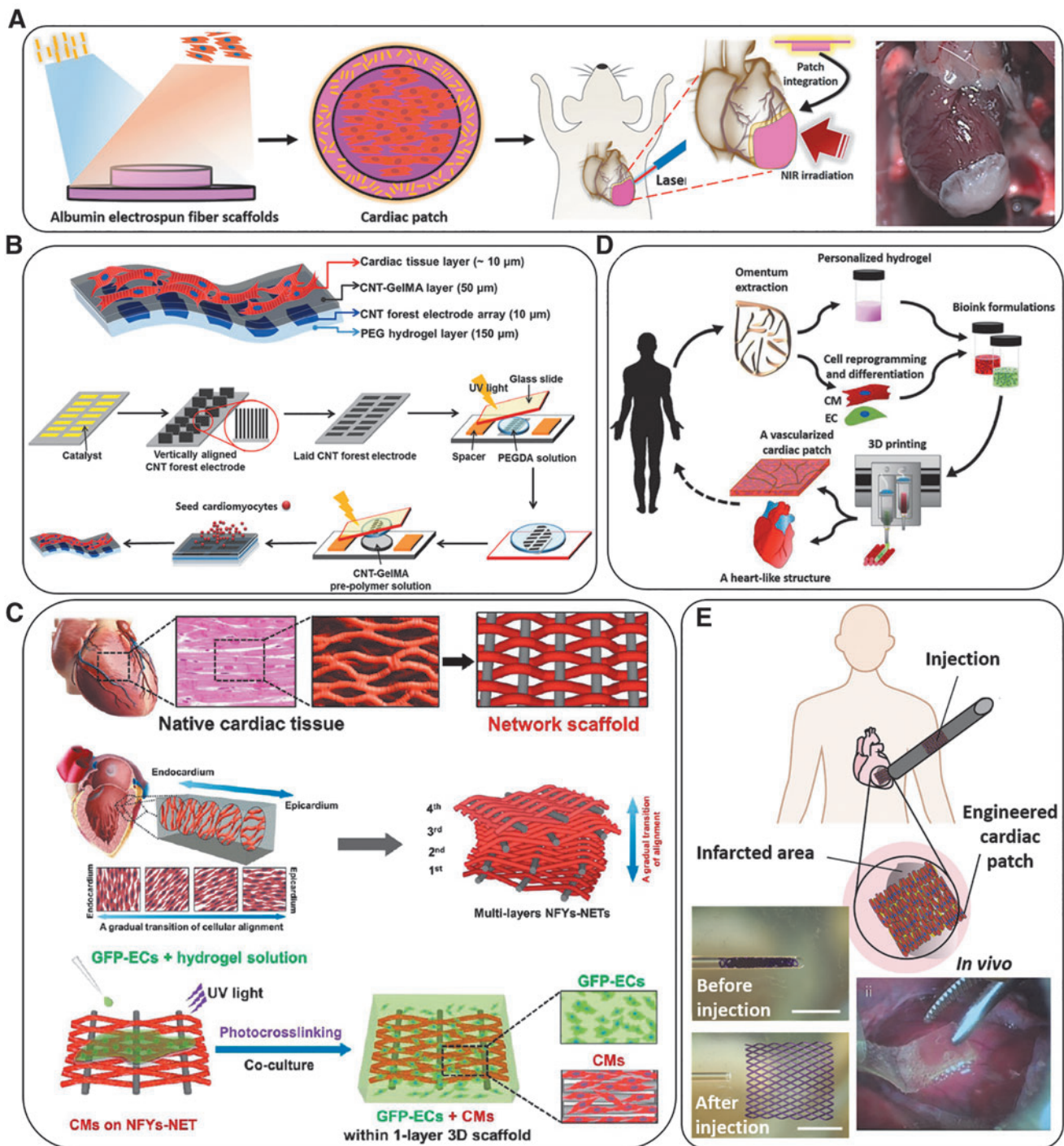


FIG. 2. Schematic overview of various types of electroconductive scaffolds used in cardiac tissue regeneration. **(A)** Overview of the concept of using a suture-free technology for the attachment of an engineered cardiac patch to the organ. The process from left to the right of the panel can be explained as: Gold nanorod adsorption; cardiac cell seeding; cardiac tissue assembly; patch location and integration by NIR; and finally, the cardiac patch after integration to a rat heart.³⁶ **(B)** A schematic illustrating the fabrication steps to produce 3D biohybrid actuators composed of cardiac tissue on top of a multilayer hydrogel sheet impregnated with aligned CNT microelectrodes.⁴⁵ **(C)** Designing a multilayered hybrid scaffold, including nanofibers and hydrogels, that can suitably mimic the native cardiac tissue structure. The first step is to design an interwoven, aligned structure, and scaffold with a network structure from nanofibers of Yarn (NFYs-NET), which possess the benefits for native cardiac tissue. The middle row demonstrates the native myocardium showing a gradual transition of aligned cell layers from the endocardium to the epicardium and shows schematics of multiple layers of NFYs-NETs assembled with a gradual orientation transition. The bottom row shows the fabrication process of one-layer 3D NFYs-NET/GelMA hybrid scaffolds and subsequent CMs cultivation. A single-layer hybrid 3D scaffold is formed through encapsulating a single NFYs-NET layer within a GelMA hydrogel shell after photocrosslinking with UV-radiation. **(D)** Schematic concept of using a cell-laden hydrogel bioink originating from the patient's own cells that are reprogrammed to become pluripotent and then differentiated to CMs and endothelial cells and encapsulation within the hydrogel for 3D bioprinting functional cardiac tissue (so-called personalized tissue regeneration).⁴⁶ **(E)** Schematic concept of the application of an engineered functional and injectable cardiac patch through a shape/memory scaffold. The scaffolds recover their initial shape following injection. An image of the minimally invasive implanted injectable cardiac patch on the porcine heart without open-heart surgery is also shown.⁴⁷ 3D, three-dimensional; CMs, cardiomyocytes; CNT, carbon nanotube; GelMA, gelatin methacryloyl; NIR, near infrared; UV, ultraviolet.

associated with conductive polymers is their slow *in vivo* degradation rate (more than 8 weeks), which makes them inappropriate candidates due to their risk of inflammation and consequently necessitating surgical removal.^{4,41–43} Conductive polymers have also been incorporated into scaffolds to promote their contraction ability; however, their mechanical compliance (elasticity) after *in vivo* implantation has not been sufficient.⁴⁴ Therefore, in the case of electroconductive polymers, there is an unmet need to engineer conductive polymers with appropriate degradability both *in vitro* and *in vivo*, and that has fostered researchers to work on incorporating these conductive polymers at lower ratios in the design of composite hydrogels.

Many of these polymeric NMs fully degrade in the human body without exhibiting any sign of long-term toxicities; however, for some inorganic NMs, the evaluation of the potential long-term toxicity and their biological fates is essential for safety purposes.³⁷

In a research study, Liang et al.²⁸ reported an adhesive, 3D printable and rapidly bondable electroconductive polymeric hydrogel as a cardiac patch that can be conveniently employed onto an injured heart without any external harm from sutures or light stimulation, or any adverse liquid leakage. Their functional and translatable sutureless strategy could be a promising method to address the challenges associated with the implementation of cardiac patches onto the heart in human clinical trials.

Table 2 summarizes the most recent and commonly used type of electroconductive nanobiomaterials and their composition for CVD therapy along with the promising properties of these systems. Most of these instances, such as electrospun nanofibrous scaffolds, hydrogels, 3D printed constructs, and nanostructured films, can appropriately mimic the ECM substrate of the native cardiac tissue, which can effectively surround, interact and affect CMs adhesion, growth, proliferation, and differentiation while providing an appropriate substrate for mechanical integrity of the cardiac tissue. Numerous studies have reported different nanobiomaterials that can mimic the mechanical and biological properties of a native cardiac structure while improving the synchronous beating of CMs and subsequently achieve better regeneration of the myocardium, reducing the infarcted area. In this section, we provided a comprehensive overview and lots of insight into the most recent studies that introduce various potential electroconductive nanobiomaterials to regenerate the function of cardiac tissue.

Neural tissue engineering

Quantum dots. Quantum dots (QDs) are synthetic nanoscale semiconductor crystals 2–10 nm in diameter made of different core components, such as cadmium selenide or cadmium telluride, indium phosphide, or indium arsenide usually coated with zinc sulfide. This structure gives QDs a superior photophysical potential and also the ability to cross the blood/brain barrier (BBB) and directly reach the brain tissue. The BBB is a semipermeable structure (consisting of endothelial cells, astrocytes, and pericytes) that protects the central nervous system (CNS) and is noticeably selective in allowing molecules to pass into the CNS. This selectivity tremendously limits drug delivery to the brain and to the CNS in general. Additionally, there is a very high electrical resistance across the BBB due to intercellular tight junction complexes that keep

endothelial cells together. These junctions are composed of different proteins, including but not limited to claudins, ZO-1, and occludin. This structure, along with the physiological and electrical mechanisms, prevent pathogens and toxins from entering the brain and, in turn, limits the brain uptake of therapeutic compounds.⁶⁵ NP-mediated drug delivery has been considered as a method to help drugs cross the BBB. However, most NPs are no exception and cannot cross the BBB. Therefore, strategies have to be conducted to make it possible for some of the NPs to cross the BBB, and these strategies take advantage of the underlying physiological mechanisms. It has been said that NPs smaller than 200 nm have a higher chance to cross the BBB, which is the limiting size of the NPs to go through endocytosis through the clathrin-mediated mechanism.⁶⁵ Saccharide-based carbon quantum dots (CDs), on the other hand, can cross the BBB in different vertebrates⁶⁶ and are novel nanocarriers introduced for drug delivery. In the past, there have been concerns about QDs and their use *in vivo* due to their intrinsic toxicity. CDs are a green, carbon-based version of QDs, for drug delivery across the BBB. The low toxicity of CDs compared with other QDs is due to a lack of metal elements. CDs can be made by oxidizing the double bonds on raw carbon powder (a top-down approach) or as polymeric structures made of several monomeric units of, for example, citric acid (C₆H₈O₇) and amines bound together through covalent and hydrogen bonds (a bottom-up approach).^{67,68}

Gold nanoparticles. AuNPs are composed of nanoscale clusters of AuNPs and are formed from the reduction of gold salts. These nanoparticles can be coated with a variety of ligands to acquire different functionalities.⁷² AuNPs are used both for drug delivery through the BBB to treat CNS infections and in neurodiagnostics. For the critical demarcation of brain tumors, AuNPs have been shown to be among the best metal-based nanoparticles to improve the capabilities of contrast-enhanced magnetic resonance imaging (MRI). AuNPs are safe contrast agents for “multimodality” neuroimaging to enhance tumor edges and also to evaluate postoperative precision in neurosurgeries.^{73,74}

Colloidal AuNPs have low toxicity and a suitable architecture that allows them to cross the BBB or the blood/brain tumor barrier. Poly(ethylene glycol) (PEG)-coated AuNPs provide a unique drug delivery system without requiring any molecular drug modifications. Additionally, the surface of AuNPs can be transformed to improve targeting glioblastoma cells, which consequently, further improves drug delivery. To transform the surface of AuNPs, they are coated with thiolated PEG or liposomes. These coatings help AuNPs evade the immune system.⁷⁵ AuNPs are only one of several modalities to transfer drugs into cells. Kang et al.⁷⁰ have nicely presented a comprehensive list of nanomedicines targeting the CNS along with their nanocarriers.

Nanoneedles and nanowires. Nano-sized “needles” can be used as nanoelectrodes and provide high-quality neurophysiological recordings of neurons and neural networks. Nanoneedles of 200–300 nm in diameter can reach the depth of the cell nucleus and make subcellular surgery *in vivo* possible.⁷⁶ Figure 3A shows the usability of nanoneedles and nanowires.

Nanowires can be produced in broad ranges based on classic semiconductors and can provide optimal control over

TABLE 2. NANOENGINEERED ELECTROCONDUCTIVE SCAFFOLDS FOR CARDIOVASCULAR TISSUE REGENERATION

Type of conductive scaffold	Composition	Fabrication techniques	Measurement device	Cellular type	Properties (with a focus on electrical properties and cellular activity)	Ref.
Hydrogels	Ge/IMA–AuNRs	Simple mixing of GelMA with AuNRs, sonication, and UV photocrosslinking	AFM and LCR meter A custom-made electrical field stimulation chamber	NRVCMs	Embedding AuNRs significantly promoted cellular retention and the expression of cardiac-specific markers, including SAC, cTnI, and Cx43 gap junctions Lower excitation voltage threshold for hydrogels embedded with AuNRs The EIS measurement demonstrated the inclusion of AuNRs and significantly reduced the electrical resistance of GelMA–GNR ($2.5 \pm 0.03 \text{ k}\Omega$ at 20 Hz) as compared with both pristine GelMA (5%) ($12.65 \pm 5.21 \text{ k}\Omega$ at 20 Hz) and GelMA (20%) ($21.58 \pm 3.56 \text{ k}\Omega$ at 20 Hz) hydrogels	29
Hydrogels/hybrid nanocomposite	Ge/IMA–PANI	Interfacial polymerization Simple blending and crosslinking using Irgacure	Three electrode system EIS using a custom-made resistance-test-chip Direct current resistance system	Murine mesenchymal progenitor cells	Can be printed in complex user-defined geometries using digital projection stereolithography Useful in developing next-generation bioelectrical interfaces Significant decrease in resistance (increase in conductivity) by doping PANI. GelMA–PANI showed resistance of $165.56 \pm 5.97 \Omega$ compared with pristine GelMA $508.60 \pm 6.84 \Omega$ The impedance of GelMA–PANI ($2.9 \pm 0.3 \text{ k}\Omega$) was significantly lower than pure GelMA sample ($6.9 \pm 0.7 \text{ k}\Omega$)	48
Hydrogels	Ge/IMA–PEDOT:PSS	Filtered, sonicated, blended, crosslinked	EIS workstation	C2C12 myoblasts	In an <i>ex vivo</i> experiment, the threshold voltage to stimulate contraction of abdominal tissue decreased compared with GelMA control Enhanced conductivity and biocompatibility At lower frequencies (similar to electroactive biological tissues, 1 Hz), the resistivity of GelMA:PEDOT:PSS was lower than pure GelMA hydrogel at 1 Hz and impedance decreased from 449.0 k Ω for pure GelMA to 261 k Ω for GelMA:PEDOT:PSS hydrogel	49
Biohybrid hydrogel arrays	Ge/IMA–CNTs	Encapsulation of microelectrodes into hydrogels, and then UV crosslinking	A custom-made two carbon electrode system	Neonatal rat ventricular CMs	CNT microelectrode-integrated hydrogels exhibited excellent anisotropic electrical conductivity Aligned CNTs provide homogeneous cell organization with improved cell-to-cell coupling and maturation	45

(continued)

TABLE 2. (CONTINUED)

Type of conductive scaffold	Composition	Fabrication techniques	Measurement device	Cellular type	Properties (with a focus on electrical properties and cellular activity)	Ref.
Hybrid hydrogels	GeIMA-rGO	Simple mixing and UV crosslinking	EIS and a custom-made platinum wire electrode system	Neonatal rat ventricular CMs	Significantly enhanced the electrical conductivity and mechanical properties Stronger CM's contractility and faster spontaneous beating rate on rGO-GeIMA hydrogels At the same frequency (100 Hz), the GeIMA-rGO hydrogels showed significantly lower impedance of 1.2 k Ω than those of pristine GeIMA hydrogels (6 k Ω)	50
Hydrogel	Gelatin (porcine skin)-SWCNTs	Mixing, sonication, and GP crosslinking	Impedance test using a precision LCR meter	H9c2 rat cardiomyoblasts	Enhanced cellular electrical excitability More mature cardiac phenotype in H9c2 Gelatin-SWCNTs showed mechanical strength with low electrical resistance and high thermal conductivity Highest conductivity (at low frequencies) was observed at 0.9% w/w SWCNTs	51
Injectable hydrogels	CS-AT-PEG	Mixing, and then PEG-DA crosslinking agent	Pocket conductivity meter	C2C12 myoblasts and H9c2 rat cardiomyoblasts	Antibacterial and electroactive injectable hydrogels with self-healing ability High cell viability post injection Tunable release rate, and <i>in vivo</i> cell retention in conductive hydrogels Excellent candidates as cell delivery vehicle for cardiac repair Conductivity of the hydrogels was about 10 ⁻³ S/cm, which is quite close to native cardiac tissue 0.1 S/m	52
Hydrogels	MWCNTs-Collagen (type I)	Mixing and molding	Custom-made electrodes used in impedance test	Neonatal rat CMs	Simultaneous improvements in mechanical strength and electrical performance Increased rhythmic contraction of the infarcted area At lower and more biologically relevant frequencies (<100 Hz), Col-CNTs hydrogels showed lower impedance (3 k Ω vs. 5 k Ω , at 10 Hz)	53
Pericardial matrix hydrogels (PMNT gels)	Decellularized cardiac tissue-CDH functionalized MWCNT (CDH-MWCNT)	Decellularization, functionalization, and doping	Custom-made four-point probe electrical station	HL-1 CMs	CMs cultured on a PMNT scaffold triggered proliferation and significantly increased the expression of cardiac gap junctions, connexin ⁴³ The addition of CDH-MWCNT to the gel significantly increased the electrical conductivity from 0.007 to 0.015 S/cm, which is close to the native cardiac tissue conductivity of 0.1 S/cm	54

(continued)

TABLE 2. (CONTINUED)

Type of conductive scaffold	Composition	Fabrication techniques	Measurement device	Cellular type	Properties (with a focus on electrical properties and cellular activity)	Ref.
Nanoporous scaffolds	Polyurethane containing AP segments (AP-PU), PCL	Salt leaching/compression molding technique	Four-point probe electrical station	Neonatal rat CMs	Scaffolds supported CM's adhesion and growth with more extensive effect on the expression of the cardiac genes involved in muscle contraction and relaxation (troponin-T) and cytoskeleton alignment (actinin-4) The conductivity of the composite scaffold was $10^{-5} \pm 0.09$ S/cm (which is in the range of semiconductor materials $10^{-2} - 10^{-6}$ S/cm) Conductivity preserved for 120 h postfabrication in cell media	55
Nanofibrous scaffolds	GeIMA-Bio-IL	Electrospinning, and then physical conjugation	Two-probe electrical station	Coculture of neonatal rat CMs and CFs	Adhesive and sutureless scaffolds because of the formation of ionic bonding between the Bio-IL and native tissue Overexpression of the gap junction protein connexin 43 in GeIMA-Bio-IL scaffolds Minimize cardiac remodeling and preserve normal cardiac function The conductivity of 10% (w/v) GeIMA-Bio-IL scaffolds was increased from 0.023 ± 0.002 to 0.138 ± 0.012 S/m by increasing Bio-IL from 33% to 66%	56
Nanofibrous scaffold	PLGA-PPy	Electrospinning	Cyclic voltammetry measurements	iPS-CMs	The PLGA-PPy fibrous scaffold is capable of delivering direct electrical and mechanical stimulation to iPS Increased expression of cardiac markers No cytotoxic effect on iPS Fiber scaffolds are capable of dynamic mechanical actuation	57
Electrospun nanofibrous scaffold	PVDF-TrFE	Electrospinning	Deposited gold electrodes to AM systems differential AC amplifier	Neonatal rat left ventricular derived CMs, and hiPSC-CMs	The scaffolds perform as sensors for tissue construction from $\sim 10^5$ of CMs Contractions of CMs induced mechanical deformations, which resulted in measurable electric voltage	13
3D macroporous scaffolds	PEDOT:PSS	Ice-templating method	Custom-made OECTs	Mouse fibroblasts (3T3-L1)	Tunable pore size and morphology Enabled precise control over the conformation of adsorbed proteins (e.g., fibronectin) Electroactive cell adhesion and proangiogenic capability	58
Hybrid electrospun nanofibrous scaffold	Albumin-AuNRs	Electrospinning, irradiation with IR laser	NA	Neonatal rat left ventricular derived CMs	Suture-free cardiac patch with a high ability to integrate to the native organ AuNRs absorbs the IR light and converts to energy, which provides attachment to the heart Reduce the risk of injury to the myocardium	36

(continued)

TABLE 2. (CONTINUED)

Type of conductive scaffold	Composition	Fabrication techniques	Measurement device	Cellular type	Properties (with a focus on electrical properties and cellular activity)	Ref.
Hybrid/composite patches	PGS-collagen type I-PPy	Evaporation method	Four-point probe electrical station	H9c2 cardiomyoblast rat cells	High viability of CMs after 1 month seeding on cardiac patches Incorporation of a small molecule (3i-1000) in cardiac patches induced CM proliferation High blood wettability and drug release PGS/Col/5%PPy showed significantly higher conductivity of 0.06 ± 0.14 S/cm	59
Hybrid polymeric scaffolds	CNTs-PEGDM-124 polymer	Dispersion, molding, UV crosslinking	Ionic conductivity meter	Neonatal rat ventricular CMs	Conductive polyester-CNT scaffolds presented greater tissue maturity 124 polymer-CNT scaffolds demonstrated improved excitation threshold in materials with 0.5% CNT content (3.6 ± 0.8 V/cm) compared with materials with 0% (5.1 ± 0.8 V/cm) and 0.1% (5.0 ± 0.7 V/cm) CNT-porogen mixture had ionic conductivity of 0.08 ± 0.01 mS/m, compared with 0.06 ± 0.01 mS/m for porogen without CNTs and 0.06 ± 0.01 mS/m for DI water	60
3D hybrid composite scaffolds (NFYs-NET within a hydrogel shell)	PCL, SF, and CNTs, and GelMA	Weaving technique for fabrication of NFYs-NET, and encapsulation of NFYs-NET layer in GelMA following by crosslinking	Van Der Pauw DC four-probe method	Coculture of CMs (from neonatal rat) and endothelial cells	Mimicking the anisotropic cardiac structure and controlling the cellular alignment and elongation Enhanced CM's maturation in a 3D environment as well as suitable endothelialization The conductivities of these NFYs-NET samples ranging from 6.5×10^{-5} to 8.1×10^{-5} S/m	61
Thin film (patch)/substrate	Single-walled CNTs/collagen substrates	Assembly of IDs through disposition technique	HP 34401A multimeter, and two-probed electrical station	NRVMs	Enhanced CM's adhesion and maturation Addition of CNTs remarkably increased ID-related protein expression and enhanced ID assembly, and CNTs remarkably accelerated gap junction formation functionality CNTs enhanced ID assembly Col-CNT (0.1 mg/mL) showed significantly greater conductivity of $(1.72 \pm 0.31) \times 10^{-9}$ S compared with the conductivity of pristine collagen as $(4.73 \pm 0.25) \times 10^{-12}$ S Conductivity significantly depends on CNT concentration, $(1.9 \pm 0.1) \times 10^{-11}$ S for Col-CNT (0.05 mg/mL), while $(1.77 \pm 0.25) \times 10^{-6}$ S for Col-CNT (0.2 mg/mL)	62
Films	PPy-chondroitin sulfate-dodecylbenzene sulfonic-sodium paratoluene-sulfonate	Electrochemical polymerization-doping	Cyclic voltammetry with a potentiostat	CPCs isolated from adult mice hearts	Controlling the surface properties of conductive PPy polymers can greatly influence the viability of CPCs All different dopants demonstrated similar C-V profiles, which showed a capacitive response that is typical for PPy films	63

(continued)

TABLE 2. (CONTINUED)

Type of conductive scaffold	Composition	Fabrication techniques	Measurement device	Cellular type	Properties (with a focus on electrical properties and cellular activity)	Ref.
3D printed scaffold	PCL-CNTs	Mixing, sonication, and then 3D printing	Four probe method low Resistivity Meter	H9c2 rat cardiomyoblasts	1% CNT showed the optimal conductivity and stiffness for the proliferation of H9c2 cells PCL-CNTs are enzymatically biodegradable after cardiac tissue formation Conductivity of PCL-CNTs increased with increasing CNT content, 1.2×10^{-6} S/cm for PCL-5% CNTs (w/w) compared with pure PCL, which is less than 10^{-15} S/cm	64
3D painted hydrogel scaffold	PPy-dopamine-PEGDA-Gelatin	3D painting	Four-point probe electrical station EIS	L929 mouse fibroblasts, and BMSCs	HPAE/PPy conductive and adhesive hydrogel can be 3D painted and rapidly bondable onto the surface of the injured heart without adverse liquid leakage Reconstruction and revascularization of the infarcted myocardium was remarkably improved Conductivity of $9.16 \pm 0.19 \times 10^{-5}$ S/cm for HPAE-Py (50%)/Gelatin compared with $8.04 \pm 0.28 \times 10^{-6}$ S/cm for Gelatin	28
Cryogel	Ppy NPs-GelMA-PEG	Additive component method, then mixing, and finally crosslinking through a muscle-inspired dopamine	Multifunctional digital four-probe tester	Neonatal rat ventricular CMs	Enhanced myocardium regeneration due to the dopamine crosslinker, which facilitates the homogeneous distribution of PPy in cryogel Excellent synchronous contraction by increasing the expression of α -actinin and CX-43 Elevated fractional shortening and ejection fraction, and reduction of infarct size	44
Injectable shape-memory scaffold	POMAC	Combination of soft-lithography and injection molding	A custom-made EIS workstation	Neonatal rat CMs	Successful minimally invasive delivery of human cell-derived patches to the epicardium of porcine heart was achieved (Fig. 2E) Full recovery of the shape following injection without affecting CM's viability and function	47

124 polymer, poly octamethylene maleate (anhydride) 1,2,4-butanetricarboxylate; 3D, three-dimensional; AFM, atomic force microscopy; AP, aniline pentamer; AuNRs, gold nanorods; Bio-IL, bio-ionic liquid; BMSCs, bone marrow stromal cells; CDH, carbodihydrazide; CDFs, cardiac fibroblasts; CMs, cardiomyocytes; CNTs, carbon nanotubes; CPCs, cardiac progenitor cells; CS-AT, chitosan-graft-aniline tetramer; cTnI, cardiac troponin I; Cx43, connexin43; DI, deionized; EIS, electrochemical impedance spectroscopy; e-SiNWs, electrically conductive silicon nanowires; GelMA, gelatin methacryloyl; GP, Genipin; hiPSC-CMs, human induced pluripotent stem cell-derived CMs; HPAE, hyper-branched polyamine-ester; IDs, intercalated discs; iPS-CMs, induced human pluripotent stem cell-derived CMs; IR, infrared; MWCNTs, multiwall carbon nanotubes; NFYs-NET, nanofiber yams network; NPs, nanoparticles; NRVCs, neonatal rat ventricular cardiomyocytes; NRVMs, neonatal rat ventricular myocytes; OECTs, organic electrochemical transistors; PANI, polyaniline; PCL, poly(ϵ -caprolactone); PEDOT:PSS, poly(3,4-ethylenedioxythiophene):poly(styrenesulfonate); PEG, poly(ethylene glycol); PEG-DA, dibenzaldehyde terminated poly(ethylene glycol); PEGDA, poly(ethylene glycol) diacrylate; PEGDM, poly(ethylene glycol) dimethyl ether; PGS, poly(glycerol sebacate); PLGA, poly(lactic-co-glycolic acid); POMAC, poly(octamethylene maleate (anhydride) citrate); PPy, Polypyrrole; PVDF-TrFE, poly(vinylidene fluoride-trifluoroethylene); rGO, reduced graphene oxide; SAC, sarcomeric α -actinin; SWCNTs, single-walled carbon nanotubes; UV, ultraviolet.

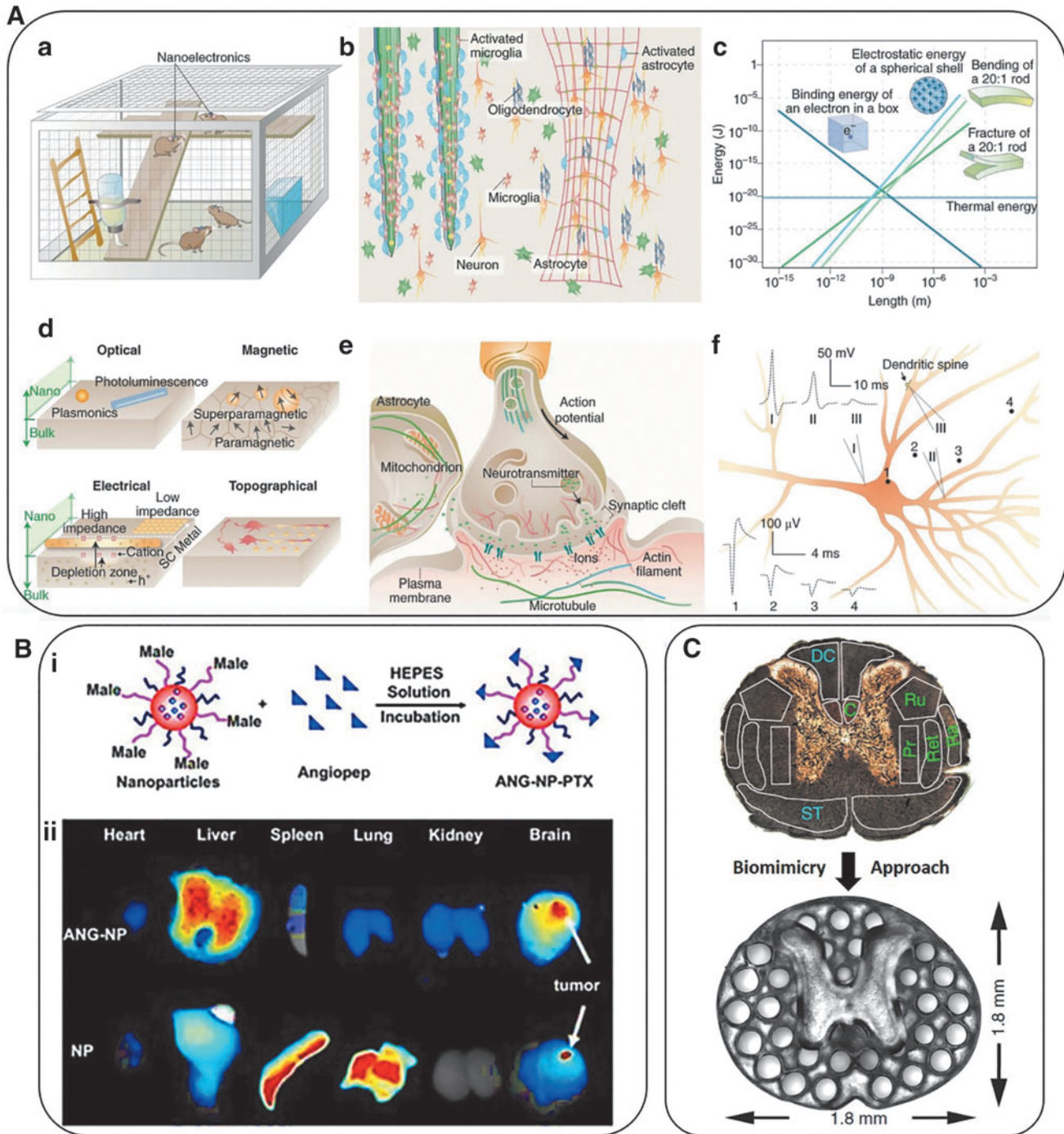


FIG. 3. (A, a) Nanoelectrodes as a minimally invasive wireless device for recording neuronal activities in model animals. (b) Left side of the photo shows traditional bulk implants while the right image displays nanoscale implants as an open, stretchable and flexible framework that induce fewer immune reactions. These networks allow access to many more astrocytes and microglial cells and can be activated at the surface of bulk implants. (c) Multiple forms of signal transduction in neuronal synapses. (d) The size-shrink of metal conductors or semiconductors from paramagnetic to superparamagnetic at the nanoscale compared with bulk-size properties. FETs are gated more easily when nanoscale channels are implemented. Also, nanoscale patterns can lead to a neural response that cannot be detected in a planar neural substrate. (e) The synaptic spaces and several other subcellular spaces are crowded and dynamic. Nanoscale signal transduction can record activities with much higher precision in these crowded spaces compared with traditional methods. (f) Recordings show different signal shapes and amplitudes on different sites of a single neuron. Traces 1–4 show extracellular signal recordings whereas traces I–III show intracellular recordings from micropipettes. All of panel A adopted from Taylor and Francis.⁶⁹ (B) Polymeric nanoparticles employed for targeted drug delivery. (i) Schematic representation of paclitaxel-loaded Angiopep-PEG-PCL nanoparticles. (ii) Angiopep-conjugation increased the targeting efficiency of brain tumors.⁷⁰ (C) A 3D printed implant, 2-mm in thickness, is used as scaffolding to repair spinal cord injuries in rats. The H shape in the center is the location of the spinal cord and the dots surrounding it are hollow spaces through which stem cell neural implants extend axons into the host tissues.⁷¹ PCL, poly(ϵ -caprolactone).

their position and maneuvering due to their size, diameter, and flexibility of the structure. Nanowire field-effect transistors are used as an effective method for subcellular recording. One of their variations was used for recordings in the rat cerebral cortex. This experiment opened a new chapter in the design of new electrode model systems with better and closer contact between electrodes and neurons.⁷⁶

Three-dimensional scaffolds. Biomimetic scaffolds are under intense experiments to become one of the possible treatments for neurodegenerative diseases and axonal injuries. These scaffolds are 3D synthetic hydrogel structures that can promote axonal regeneration after peripheral nerve damage. Different molecules and cells can be incorporated into the gel structure with noticeable amounts of water that make the solution and absorption of different molecules possible.

Self-assembling peptide nanofiber scaffolds (SAPNFSs) are new protective biodevices to be used as a therapeutic strategy for intracerebral hemorrhage. When SAPNS were delivered into an intracerebral hemorrhagic lesion in a rat model, they replaced the hematoma and reduced the size of the hemorrhagic lesion.⁷¹

Carbon-based smart NMs. Graphene, CNTs, and nanodiamonds (NDs) have been shown to be promising materials for the future of biotech, medicine, and nanoengineering. Among the ultimate goals of nanoengineering in the CNS are repairing and optimizing the function of the amaged brain and spinal tissues. Due to the unique structure of the CNS, today's challenge for nanoengineering is to use smart materials that can be controlled when interacting with living cells, and can also be modified as required. CNTs are one of the materials that seem ideal for this purpose.

Carbon nanotubes. The electrical conductivity of single-walled CNTs and multiwalled CNTs make them valuable when bioconductivity is required in neuronal networks. Bioconductivity and structural strength of CNTs due to their configuration and two covalent bonds, make them ideal materials to be used in nanoelectrodes for neural stimulation and also as scaffolds in tissue engineering.

Nanodiamonds. Diamond has valuable and unique characteristics, such as hardness, high mobility of electrical charge carrier ions, and high thermal conductivity.⁷⁷ Diamond nanofillers with superior hardness can reinforce any polymer matrix, which is most advantageous in creating 3D scaffolds for stem cell growth, proliferation, and differentiation. Therefore, NDs can be used to treat neural injuries and stroke.

AZTTP. 3'-Azido-2',3'-dideoxythymidine-5'-triphosphate drug-loaded magnetic nanoparticles can successfully cross the BBB to deliver drugs (such as tenofovir and vorinostat) into the brain tissue and are therefore of extreme value in neuro-HIV treatment. These achievements are currently limited to computerized simulations in *in vitro* models online. However, significant efforts are dedicated to bring this technology to future treatments of neuroHIV/AIDS and other CNS diseases.⁷⁸ Figure 3B shows the polymeric nanoparticles and their utilization in imaging.

Superparamagnetic iron oxide nanoparticles. Ultrasmall superparamagnetic iron oxide nanoparticles (SPIOs) can be used as MRI-enhancing agents in imaging of CNS inflammatory diseases, specifically in the choroid plexus. In several inflammatory brain diseases, the choroid plexus is involved. Therefore, it is crucial to have a means for the noninvasive monitoring of the choroid plexus. SPIO-enhanced MRI is a noninvasive method that can track phagocytic cells in inflammatory diseases. *In vivo* studies have shown the accumulation of SPIOs inside the choroid plexus and their uptake by myeloid cells. The iron nanoparticle used in this study was Ferumoxytol. This study confirmed the functionality of SPIOs as imaging biomarkers to examine the involvement of the choroid plexus in neuroinflammatory diseases.⁷⁹

Solid lipid nanoparticles. Solid lipid nanoparticles, when conjugated with tamoxifen and lactoferrin, are used to carry drugs like Carmustin (BNCU) through the BBB for the treatment of glioblastoma. Compared with BNCU-loaded solid lipid nanoparticles (SLNs), the combination of Tamoxifen/Lactoferrin/BNCU/SLN increased the membrane permeability for BNCU 10 times, making it a potentially promising compound for the future treatment of glioblastoma.⁸⁰

TiO₂. Around 5.5 Million Americans suffer from Alzheimer's disease (AD). Among several studies to discover a treatment for Alzheimer's, there have been researchers that show alterations in the histamine receptors in AD. It seems that histamine-modulating drugs may be a potential treatment of Alzheimer's. Antibodies to histamine and the tau protein also seem to be beneficial in the treatment of this disease. The TiO₂-nanowired delivery of cerebrolysin (a compound of multiple neurotrophic factors) has lowered the accumulation of beta amyloid plaques and phosphorylation of the tau protein in AD brains of mice and seems to be neuroprotective. In particular, when cerebrolysin was coadministered with histamine antibodies and tau antibodies, the neuroprotective effect increased. These findings suggest a strong role for TiO₂ as a nanowire for the future treatment of AD.⁷⁰

Table 3 shows a list of promising nanoengineered electroconductive scaffolds for neural tissue regeneration.

Bone tissue engineering

NMs have demonstrated promising capabilities in stimulating cell function and enhancing bone tissue regeneration. These capabilities are due to their biomimetic features and unique physicochemical, mechanical, and biological properties, which strongly differ from those found in the bulk scale. Since bone is a nanocomposite, containing nanoscale building blocks (mainly collagen fibrils and mineral hydroxyapatite plates), the use of biodegradable conductive nanocomposites is attractive for orthopedic applications.⁹⁴⁻⁹⁶ Therefore, many examples are found in literature where these NMs allow for better bone tissue regeneration, providing a better surface and physicochemical properties for osteoblast attachment and long-term function, but also have better mechanical properties for certain load-bearing conditions. As a consequence, NMs show an extreme potential in bone tissue regeneration.^{97,98}

On the other hand, it is widely known that electrical fields are present in a variety of tissues, including bone. Fukada and Yasuda first demonstrated that dry bone behaves as a

TABLE 3. NANOENGINEERED ELECTROCONDUCTIVE SCAFFOLDS FOR NEURAL TISSUE REGENERATION

Type of conductive scaffolds	Composition	Fabrication technique	Measurement device	Cellular type	Properties (with focus on electrical properties and requirements)	Disadvantages and future directions	Ref.
Composite hydrogel	OPF/CNTs/GO	Covalent embedding	34461A digital multimeter	PC-12 cells (cells from rat's pheochromocytoma), <i>Rattus norvegicus</i> , adrenal gland of rat	A synergistic effect of electrical conductivity and positive charges on nerve cells was observed Conductivity values of (3.16 ± 1.39) × 10 ⁻⁴ S/m for pure OPF hydrogel, (6.24 ± 2.70) × 10 ⁻⁴ S/m for OPF-MTAC hydrogel, and (2.96 ± 1.86) × 10 ⁻³ S/m for OPF-rGO-CNT/pega hydrogel were reposted	Enhanced proliferation and spreading of PC12 cells Great potential as conduits for neural tissue engineering NGF was used to stimulate the cells effectively	81
3D printed scaffold	PPy-polycaprolactone	EHD jet 3D printing process	Conductivity meter (pH/Ion meter S220)	hESC-NCSCs	PPy/PCL scaffolds possess conductivity ranging from 0.28 to 1.15 mS/cm depending on concentration of PPy The conductivity value for the PCL/PPy (1% v/v), which showed the most maturation of hESC-NCSCs was about 1.02 ± 0.03 mS/cm	The most attachment and differentiation of hESC-NCSCs to peripheral neurons was observed on PCL/PPy (1% v/v) Potential treatment of neurodegenerative disorders, however no <i>in vivo</i> studies were executed in this study	82
Composite microporous tube	PVDF-PCL	Cast/annealing-solvent displacement method	PFM suing AFM	RSCs	Electroconductive PVDF/PCL scaffolds have a positive effect on myelination, axon regeneration, as well as angiogenesis, which all contribute to nerve regeneration and attenuates muscle denervation	Implanted PVDF/PCL scaffolds into the 15-mm defect rat sciatic nerve model	83

(continued)

TABLE 3. (CONTINUED)

Type of conductive scaffolds	Composition	Fabrication technique	Measurement device	Cellular type	Properties (with focus on electrical properties and requirements)	Disadvantages and future directions	Ref.
Hybrid/composite	POSS-PCL-Graphene	Simple blending, sonication, and casting	EIS	Neonatal Wistar rat SCs	The percolation threshold occurred at 0.08 wt% graphene At 4.0 wt% the electrical conductivity exceeded 10^{-4} S/cm Conductivity values were reported as 8.76×10^{-14} S/cm, 3.47×10^{-11} S/cm, 1.49×10^{-7} , and 9.34×10^{-5} for pristine POSS-PCL, and POSS-PCL incorporated with 0.4, 1.6, 4 wt% graphene, respectively	OSS-PCL/graphene nanocomposites showed higher metabolic activity and cell proliferation in comparison with pristine POSS-PCL	84
Microribbons	PLGA-Graphene	Wet spinning	Four-point probe electrical station	Human neuroblastoma cell line SH-SY5Y	Conductivity value of $0.15 \pm 0.01 \mu\text{S/m}$ for pristine PLGA, while incorporation of 1 wt% Gr nanosheets induced a conductivity of 0.42 ± 0.03 S/m	Lack of <i>in vivo</i> studies that show these PLGA/Graphene microribbons can stimulate neural stem cell function	85
3D Braided filaments	SF-PCL-CNFs	Home-made coating system	Impedance analyzer	N2a mouse neural crest-derived cell	By increasing the CNF in the coating, the electrical impedance decreased up to 400Ω The lowest impedance of $316 \pm 3.42 \Omega/\text{mm}$ was observed for the highest concentration of CNFs at a frequency of 20 MHz	Lack of <i>in vivo</i> studies Potential use for successful regeneration of a 15–20 cm nerve gap	86
Hybrid electrospun scaffold	PHA-Graphene-gold nanoparticles	Electrospinning	NA	PC-12 cells and SCs	Conductivity measurements were not performed	PHA-RGO-Au scaffolds prominently endorsed SCs proliferation and migration No data on the conductivity values of the scaffolds were reported Lack of enough data to conclude the ability of the engineered scaffolds in peripheral nerve regeneration	87

(continued)

TABLE 3. (CONTINUED)

Type of conductive scaffolds	Composition	Fabrication technique	Measurement device	Cellular type	Properties (with focus on electrical properties and requirements)	Disadvantages and future directions	Ref.
Hybrid nanocomposite scaffold	PVDF-GO	Nonsolvent induced phase separation method	EIS-ARSTAT 2273,	Rat neuronal PC-12 cells	Incorporation of GO nanosheets into the PVDF scaffold simultaneously enhanced β -phase fraction, piezoelectricity, and electrical conductivity Incorporation of 1 wt% GO into PVDF, reduced impedance value from 804.6 ± 53.4 to $105.7 \pm 32.45 \Omega$	PVDF-GO scaffolds significantly promoted PC12 cell proliferation, compared with pristine PVDF scaffold	88
CNT-based scaffolds	Graphene sheets	Chemical vapor deposition, Electric arc discharge, Laser ablation	Single-cell patch clamp recording	Neurons (PC-12 cells)	Sheets of graphene formed into cylinders that can be single walled, double walled, and multiwalled ⁷¹ Neural interfaces formed as a microchip on a quartz substrate using plasma etching and photolithography Flexibility and bioconductivity CNT-based scaffolds used as substrates for neural cell growth	Lack of solubility in aqueous media; Surface modification with hydrophilic molecules is the method used to overcome this disadvantage ⁸⁹	90,91
Substrate-bound transistors and electrodes	Silicon nanowires and graphene	Evaporation	STM	Neurons	There are three terminals for transistors: source, drain, gate Electric field is generated by voltage applied to the gate ⁹² An electrically neutral area is required around transistors and microelectrodes and also a cascade of enzymes to transmit signals ⁹³ Tumor enhancement for imaging through transferring excitatory stimuli	Electroactivity of different molecules in the brain that can interfere with microelectrodes and sensors; Nafion barriers are used to decrease impulse interfering ⁹³	69

CNFs, carbon nanofibers; EHD, electrohydrodynamic; GO, graphene oxide; hESC-NCSCs, human embryonic stem cell-derived neural crest stem cells; N2a, neuro 2A; NPF, nerve growth factor; PFM, piezoresponse force microscopy; PHA, polyhydroxy] alkanolate; POSS, polyhedral oligomeric silsesquioxane; OPF, oligo(poly(ethylene glycol) fumarate); RSCs, rat Schwann cells; SCs, Schwann cells; SF, silk fibroin; STM, scanning tunneling microscope.

piezoelectric material in the classic sense, hence mechanical stresses result in electric polarization. On the other hand, the study of the dielectric and piezoelectric properties of fully hydrated bone raises some doubts as to whether wet bone is piezoelectric at all at physiological frequencies. Besides, both dielectric and piezoelectric properties of bone depend strongly upon frequency. Moreover, conductivity values of bone tissues are strongly dependent on the type of bone (i.e., bone density, bone architecture, water content, etc.); for instance, in a study, this value was measured as 9.1 mS/m for cortical bone, whereas the conductivity of bone marrow was about 0.23 S/m (both at 100 kHz).⁹⁹ Another study reported the values of 0.043 ± 0.024 , 0.02, and 0.29 ± 0.031 S/m for cancellous bone, cortical bone, and subchondral bone, respectively (all at 20 Hz).¹⁰⁰ Consequently, electrical stimuli play an essential role in a wide array of biological processes involved in bone regeneration, such as angiogenesis, cell signaling, or cell division, among others. All of these processes are mediated by a variety of subcellular cues, including protein distribution, gene expression, or metal ion content. Since all of them can be easily controlled by the modulation of an applied electric field,¹⁰¹ electroactive or bioelectrical tissue engineering is able to provide biomaterials with electroconductive properties, becoming a field of study which has gained much attention in an attempt to boost the therapeutic efficacy of NMs destined for use in bone integration strategies.²

Besides, bioelectricity properties can be incorporated into NMs with chemical and mechanical properties similar to those of native ECM through different methods with the general aim to improve cell adhesion, viability, proliferation, and ultimately function.¹⁰² Over the past few decades, many studies have been carried out to identify the perfect combination of osteoblasts and other bone-associated cells and electroconductive nanostructures able to act as biomimetic templates for enhanced bone regeneration. However, little success has been achieved in translating these materials to the clinic.^{103,104} In this section, the recent progress in the application of electroconductive NMs for osteogenic regeneration is presented, with special focus on biodegradable or biocompatible materials.

One of the most widely known examples is polyvinylidene fluoride (PVDF) and polyvinylidene fluoride/trifluoroethylene (PVDF-TrFE), attractive materials for making functional scaffolds for bone tissue engineering applications due to their excellent piezoelectricity, composition dependent dielectric properties, and AC conductivity, as well as a good biocompatibility. Electrospun PVDF and PVDF-TrFE scaffolds can produce electrical charges during mechanical deformation, which can provide necessary stimulation for repairing bone defects. Therefore, the mats promote the adhesion, proliferation, and differentiation of bone cells on their surfaces, with such effects deriving from the formation of electroactive, polar β -phase, which has piezoelectric properties. In this polar phase, the planer all-trans (TTTT) conformation and the H and F atoms are attached in the chain in such a way that the dipole moments associated with the two C–H and two C–F bonds add up, hence aligning in the direction perpendicular to the carbon backbone, providing high dipole moments. Therefore, the incorporation of NMs within the fibers, in particular, clay nanoplatelets, CNTs, graphene/GO, and silica nanoparticles (SiNPs) have been reported to be very useful to induce the β -phase in PVDF.^{105,106}

The main drawbacks of the electrospinning process for making piezoelectric PVDF-based scaffolds are their small pore sizes and the use of highly toxic organic solvents involved in the synthesis process. The small pore sizes prevent the infiltration of bone cells into the framework, leading to the formation of a single cell layer on the scaffold surfaces. To overcome such drawbacks, research has aligned along with the study of modified electrospinning methods such as melt-electrospinning and near-field electrospinning.¹⁰⁶ On the other hand, graphene, GO, and functional graphene NMs, with a large variety of exciting properties that make them promising foundations on which to craft sophisticated, biomimetic, osteoinductive, synthetic scaffolds for bone regeneration, have been studied as well. For instance, GO has shown promise in the osteoinduction of stem cells, especially when coupled with growth factors. Consequently, strategies for controlling and modifying the surface chemistry of graphene materials have become increasingly sophisticated in recent years, providing access to new FGMs with clear implications in biomaterials and medicine.¹⁰⁷

Recently, Samadian et al. fabricated electroconductive electrospun carbon nanofibers (CNFs) to be used as the substrate for the electrical stimulation of bone cells. The CNFs were derived from electrospun polyacrylonitrile nanofibers by a two-step heat treatment, stabilization, and carbonization. The CNFs were seeded with a known concentration of Mg-63 cells and subsequently exposed to DC electrical fields with current intensities of 10, 50, 100, and 200 μ A. The COMSOL Multiphysics software was used to simulate the applied DC electric field applied in the fabricated electrical stimulation chamber in the presence of the seeded carbon nanofibers (SCNFs) (Fig. 4B). The simulation study confirmed the efficacy of the fabricated electrical stimulation set-up. The growth of the seeded cells significantly increased in the presence of the applied DC electric field and resulted in the highest proliferation level, $116.43\% \pm 4.76\%$, at 100 μ A. Furthermore, alkaline phosphatase (ALP) activity assays revealed a significantly increased osteogenic activity of cells, necessary for an enhanced bone healing process, as a result of the applied field. Therefore, the authors demonstrated the enhancement of conductivity in CNFs as a useful parameter for bone growth, while they also reported that the electrical sensitivity of the substrate fabricated might complement the piezoelectric characteristics of bone to facilitate growth and healing.¹⁰⁸

Alternatively, PLA scaffolds are widely used for biomedical applications, however, they have a low electrical conductivity. Consequently, there is a strong need to develop a composite scaffold combining their properties of osteogenic differentiation promotion and a 3D matrix that will allow for electrical conductivity. With the aim to solve problems such as the poor processability of conductive polymers, a novel *in situ* polymerization/thermal-induced phase separation method was used to fabricate conductive nanofibrous PLA scaffolds with PANI NPs. The simple preparation technique provided the possibility to scale-up the production of these conductive nanofibrous scaffolds. Besides, the excellent cytocompatibility of these scaffolds was evaluated by culturing bone marrow-derived mesenchymal stem cells (BMSCs) on them, showing the effect of conductive nanofibrous scaffolds on osteogenic differentiation with expression levels of ALP, osteocalcin, and runt-related transcription factor 2 during the culture of cells for up to 3

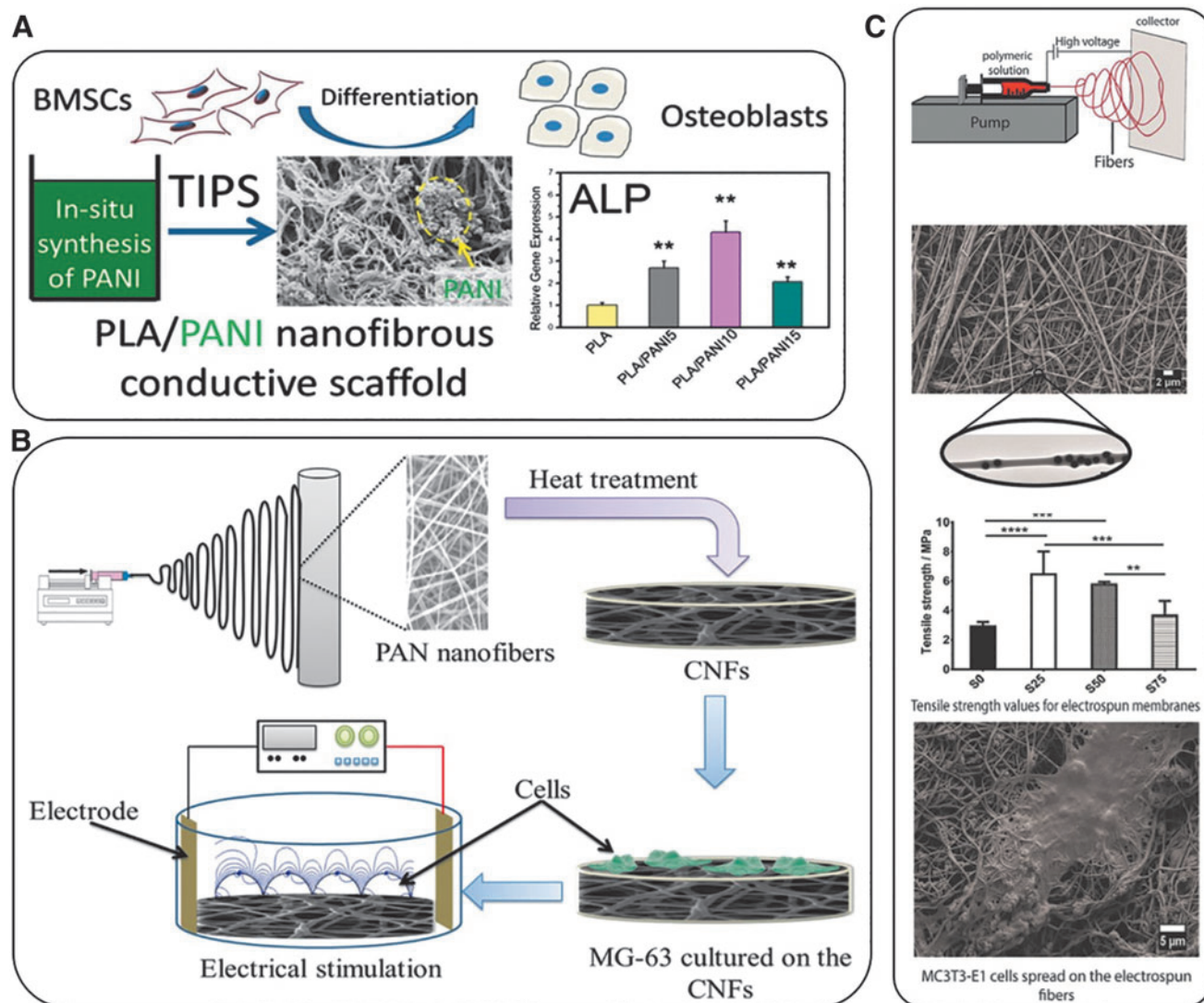


FIG. 4. Representative examples of the use of electroconductive materials for bone tissue regeneration. **(A)** Novel *in situ* polymerization/TIPS method to fabricate conductive nanofibrous PLA scaffolds with well-distributed PANI nanostructures for bone tissue regeneration.¹⁰⁹ Mean for $n=4 \pm SD$. * $P < 0.05$, ** $P < 0.01$ **(B)** Schematic representation of the experimental procedure for the fabrication of electroconductive electrospun CNFs to be used as the substrate for bone cell electrical stimulation¹⁰⁸; and **(C)** Study of the effect of the addition of Si-NPs in electrospun PCL membranes to improve the mechanical and osteoconductive properties of the layers.¹¹¹ ** $p < 0.01$, *** $p = 0.0001$, **** $p < 0.0001$. CNFs, carbon nanofibers; PANI, polyaniline; PLA, poly(lactic acid); SiNPs, silica nanoparticles; TIPS, thermal-induced phase separation.

weeks. Besides, calcium mineralization of BMSCs was studied, revealing that a moderate content of PANI NPs in the conductive nanofibrous scaffolds significantly promoted osteogenic differentiation of BMSCs for engineering bone tissues (Fig. 4A).¹⁰⁹

Similarly, Khorshidi and Karkhaneh developed a NF system, which possessed electrical conductivity due to the presence of PANI and a hydrogel fraction due to the presence of graphene NPs. The PANI-based fibers were processed through electrospinning and subsequently transformed into a 3D structure through an ultrasonication step after synthesis. The hydrogel precursor solution composed of oxidized polysaccharides, gelatin, and graphene was added to fibers and left to gel. The assessment of the natural hydrogels and hydrogel/fibers denoted that the inclusion of conducting fibers

into hydrogels increased its elastic modulus, roughness, and electrical conductivity, whereas it decreased hydrophilicity. Moreover, the results showed that the hydrogel/fiber composite better supported human osteoblast-like cell adhesion, proliferation, and morphology compared with hydrogels alone. Therefore, the presence of a gel/fiber architecture along with electrical conductivity, may lead to this kind of scaffold to be very promising for bone regeneration.¹¹⁰

Alternatively, Castro et al.¹¹¹ studied the effect of the addition of SiNPs in electrospun poly(ϵ -caprolactone) (PCL) membranes to improve the mechanical and osteoconductive properties of the layers used in bone regeneration. While PCL membranes have shown variable electrical conductivity around 4–6 mS/cm, its magnitude can be improved upon the addition of different NMs. To this end, SiNPs were first

synthesized and then suspended in PCL solutions containing the polar solvent 2,2,2-trifluoroethanol and water, together with the addition of an anionic surfactant. The nanocomposite membranes were then fabricated from the solutions through an electrospinning technique, and the effect of the materials on osteoblastic differentiation was evaluated by an *in vitro* culture of the membranes with MC3T3-E1 cells (Fig. 4C). The results indicated that the SiNPs were successfully incorporated in the interior of the PCL electrospun fibers during the electrospinning process. Their results also revealed that with increasing the amount of SiNPs, elongation at break decreased, while tensile strength and tensile modulus both increased (to a certain amount of SiNPs) and then decreased at the highest amount of SiNPs. Membranes containing SiNPs have been shown to be cytocompatible.¹¹² The results obtained demonstrated that the SiNPs were homogeneously incorporated in the electrospun fibers, resulting in an improvement of the tensile properties of the prepared materials.¹¹¹

In a different study, hybridized carbon NFs containing calcium phosphate (CaP) NPs were investigated as histocompatible nanofillers for epoxy resin. The nanosystem was produced by electrospinning a mixture solution of polyacrylonitrile and CaP precursor sol/gel, followed by preoxidation and carbonization. The continuous and long CNF/CaP was ultrasonically chopped, mixed into epoxy resin, and thermocured. The research team compared the newly synthesized system with pure CNFs with a similar ultrasonication treatment, and the shortened CNF/CaP-reinforced composites demonstrated a significant enhancement in flexural properties of epoxy composites, benefiting from the improved interfacial adhesion between CNF/CaP and resin matrix. Moreover, they also displayed excellent biocompatibility when cultured with MC3T3-E1, a mouse calvaria-derived cell line, and sustained calcium ion release, which categorized them as promising materials for bone repair.¹¹³ Similarly, Feng et al. developed a biodegradable ultraviolet (UV)-cured resin that was fabricated through a stereolithography apparatus (SLA). The formulation consisted of a commercial polyurethane resin as an oligomer, TEGDMA (trimethylolpropane trimethacrylate), as a reactive diluent, and phenylbis (2,4, 6-trimethylbenzoyl)-phosphine oxide (Irgacure 819) as a photoinitiator. The tensile strength of the 3D printed specimens was 68 MPa, 62% higher than that of the reference specimens (produced by direct casting). The flexural strength and modulus were able to reach 115 MPa and 5.8 GPa, respectively. A solvent-free method was then applied to fabricate graphene-reinforced nanocomposites. Porous bone structures (a jawbone with a square architecture and a sternum with a round architecture) and a gyroid scaffold of a graphene-reinforced nanocomposite for bone tissue engineering were 3D printed through SLA. The UV crosslinkable graphene-reinforced biodegradable nanocomposite using SLA 3D printing technology was able to significantly remove cost barriers for personalized biological tissue engineering as compared with the traditional mold-based multistep methods.^{114,115}

In a completely different approach, it is well known that the differentiation of stem cells is affected by the cell culture medium, the scaffold surface, and electrochemical signals. However, stimulation by patterned biomaterials seeded with stem cell cultures has not been extensively explored in the literature. Herein, Huang et al. studied the

effect of electrical stimulation on osteogenic differentiation of rat bone marrow-derived mesenchymal stem cells (rBMSCs) cultured on solid and nanoporous micropylramid-patterned Si surfaces. It was found that both stimulation and scaffold patterning significantly enhanced osteodifferentiation. The stimulated nanoporous micropylramid scaffolds were more promising compared with the stimulated solid micropylramid surfaces, as they significantly promoted the osteogenic differentiation of rBMSCs through the BMP/Smad signaling pathway. Notably, as compared with the unstimulated patterned biomaterials, the stimulated patterned scaffolds allowed for a significant increase in core-binding factor alpha 1, ALP, the alpha 1 chain of type I Col, osteocalcin, and osteonectin, all of which are characteristics for osteodifferentiation.¹¹⁶

Table 4 shows a list of electroconductive nanobiomaterial scaffolds used for bone tissue engineering and bone regeneration.

Tendon/skeletal muscle tissue engineering

The tendon is an intricately organized connective tissue, which connects muscles to bones to move them, and plays an important role in stress transfer and stability of the joint. Nevertheless, tendon tissue is highly prone to injury and due to the low number of cells and poor blood supply, it has a low regeneration and reparative capability.^{122,123} The surgical suturing of damaged tendons is the main clinical treatment in tendon injuries, and in most cases, auto- and allografts are used.¹²⁴ There are several major challenges in these surgical techniques such as infections, the lack of a proper number of auto and allografts, and the significant chance of allograft rejection.¹²⁵ Because of the mentioned reasons for repairing or replacing injured tendons, engineered biological substitutes with mechanical, biomimetic, and biological properties have attracted noticeable attention.¹²⁶ For instance, some bioengineering methods (such as biochemical signaling through growth factors and other biomolecules as well as electrical stimulation or mechanical stimulation), have aimed to develop biomimetic engineered skeletal muscle by mimicking the micro and nanoenvironmental cues experienced by the native muscle (Fig. 5).

In 2008, Serena et al. completed experiments to mimic neuronal activation by using a sufficient electrical field (pulse of 70 mV/cm for 3 ms). By applying this field to muscle precursor cells cultured in 3D scaffolds of collagen, they found enhanced cell proliferation in comparison with non-stimulated cultures. Although, after 10 days of implantation in mice, the number and distribution of cells did not show any difference in these two conditions.¹²⁷

On the other hand, skeletal muscle tissue includes about 45% of total body mass and is essential for generating forces for movement. In minor injury cases, skeletal muscle is able to inherently regenerate, but severe conditions like substantial traumatic injury, prolonged denervation, and myopathies lead to an irreversible loss in mass of muscle and its function. Fibrous scar tissue formation and fatty degeneration of muscle are the main results of deficiencies in regeneration.^{129,130} Autologous muscle transplantation and injection of *ex vivo* cultured muscle cells are used in the treatment of severe muscle injury, but they have shown limited achievements such as morbidity at the donor site and inadequate innervation and perfusion of the transferred muscle.¹³¹

TABLE 4. NANOENGINEERED ELECTROCONDUCTIVE SCAFFOLDS FOR BONE TISSUE REGENERATION

Type of conductive scaffold	Composition	Fabrication technique	Measurement device	Cellular type	Properties	Ref.
Electroconductive electrospun NFs scaffolds	Electrospun CNFs derived from electrospun PAN nanofibers	Two-step heat treatment regime consisting of stabilization and carbonization stages using a tube furnace	Four points probe multimeter	Mg-63 cells	Enhanced cell growth Increased osteogenic activity Conductivity of 10^{-8} S/cm	108
	Nanofibrous PLA scaffolds with well-distributed PANI nanoparticles	<i>In situ</i> polymerization/TIPS	Electrochemical workstation (CH Instruments)	BMSCs	Enhanced osteogenesis, quicker mineralization, osteogenic differentiation promotion Conductivity of 0.004–0.032 S/cm (depending on the PANI concentration)	109
	PANI and hydrogel fraction owing the presence of graphene nanoparticles	Electrospinning and ultrasonication	Two-point probe method (2601A; Keithley Instrument)	Human osteosarcoma cells (MG-63)	Enhanced cell adhesion and proliferation Conductivity of 9 ± 2 (hydrogel) and 10 ± 1 (hydrogel/fiber) μ S	110
	SINPs in electrospun PCL membranes	Electrospinning	Electrochemical workstation	MC3T3-E1 osteoblastic cells	Enhanced biocompatibility	111
	Hybridized CNF/CaP	Electrospinning, preoxidation and carbonization	Electrochemical workstation	MC3T3-E1, a mouse calvaria-derived cell line	Improved mechanical properties High biocompatibility Sustained calcium ion release	117
Nanoparticle-reinforced resins	Graphene-reinforced polyurethane resin	Stereolithography		Porous bone structures	Graphene-like (2700 S/cm) Removal of cost barriers for personalized biological tissue engineering	114
Nanopatterned surfaces	Nanoporous micropyramid-patterned Si surfaces	Etching P-type Si wafers	Electrically stimulated within a bioreactor (AFG1022 electrical signal generator)	rBMSCs	Enhanced osteo differentiation Silica-like (5×10^{-12} S/cm)	116
Hydrogels	MAETAC and SMA, were incorporated into PEGDA hydrogels	Chemical synthesis and combination		MC3T3-E1	Enhanced osteoblast proliferation Upregulation of ALP activity Upregulation of osteogenic marker genes and growth factor expression	118
Foams	PP foam	Injection molding	Piezoelectric tests	Osteoblasts cells	Promotion of piezoelectric response High biocompatibility Enhanced cell proliferation	119
Composite scaffolds	Piezoelectric, porous BaTiO ₃ and HA composite scaffolds	3D printing process	Piezoelectric tests	Mouse calvaria preosteoblast MC3T3-E1 cells	Cytocompatibility Improved cell attachment Bone mimicking properties	120
	Highly porous barium titanate-based scaffolds coated by Gel/HA nanocomposite	Foam replication method	Piezoelectric tests	MG-63 cell line	Biocompatibility Enhanced bone proliferation	121

ALP, alkaline phosphatase; BaTiO₃, barium titanate; CaP, calcium phosphate nanoparticles; HA, hydroxyapatite; MAETAC, 2-(methacryloyloxy)ethyl-trimethylammonium chloride; NF, nanofiber; PAN, polyacrylonitrile; PLA, poly(lactic acid); PP, piezoelectric polypropylene; rBMSCs, rat bone marrow-derived mesenchymal stem cells; rBMSCs, Seeded carbon nanofibers; SiNPs, silica nanoparticles; SMA, sodium methacrylate; TIPS, thermal-induced phase separation.

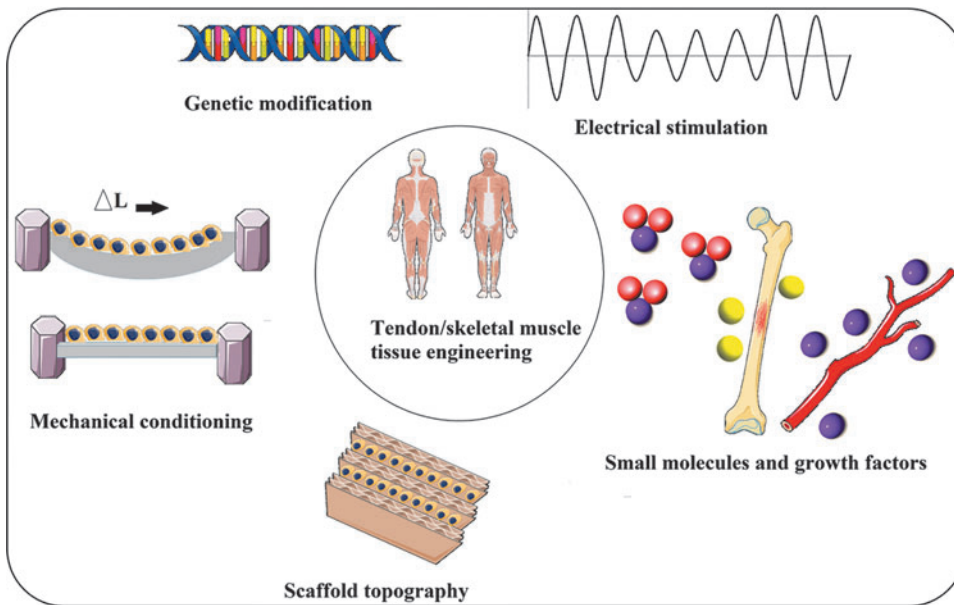


FIG. 5. Overview of bio-engineering approaches for skeletal muscle tissue engineering, redrawn from Nakayama et al.¹²⁸

Tissue engineering strategies for tendon/skeletal muscle repair that use designed biomaterials potentially offer solutions to several limitations of current therapies. Physical and chemical cues can be provided by such biomaterials to host (transplanted) muscle cells for enhancement of their survival, promote their functional maturation, recruit host nerves and vasculature into the defect site, and reduce the body response against foreign agents.¹²⁹

It is well known that surface properties of biomaterials play an essential role in the interactions between cells and substrates. In scaffold design, the ability to keep cells on the surface rather than within the hydrophobic structure is still challenging. Thus, several techniques for surface treatment have been developed to fabricate substrates with high potential for cell attachment. These techniques include ion implantation, alkaline treatment, electrochemical etching, coating with plasma spray, anodization, and biomimetic treatments.¹³² Electrical stimulation has been used in several clinical trials to significantly help in functional recovery, muscle regeneration, and better tissue repair in patients. Different parameters have been studied such as current amplitude, stimulation frequency, and time. It has been reported that lasting low-frequency electrical stimulation has effects on the growth and differentiation of myoblasts by duplicating some bioelectric signals.^{4,133–135} Fabricating substrates from materials with electroactive properties are suitable for the adhesion and growth of cells and can make possible the stimulation of cellular activity through electrical transfer.¹³⁶ For a suitable environmental stimulus to promote healthy cell function and regeneration of tissue, it is required to develop scaffolds with all requirements, such as chemical, electrical, and mechanical properties. Tissue conductivity (nerve, cardiac, ventricular muscle, lung, and skeletal muscle) lies in an ordered manner in between 0.03 and 0.6 S/m.⁹ From a biomimetic view, a designed skeletal muscle scaffold must show indigenous-like structural attributes, including aligned myofibers all over a relevantly large tissue volume.¹³⁷

Another technique is using an *in vitro* assay for the differentiation of muscle tissues, and implantation of muscle

pioneer cells on a matrix. New muscle tissue is expanded *in vitro* through controlling the environmental conditions to promote cell differentiation, with the process being extremely related to the substance acting as the scaffold for cells.¹³⁸ To date, a few research studies have been completed to innervate a construct before implantation; however, many researchers have applied external electrical stimuli to promote myotube development.¹³⁹ The incorporation of electrically conductive substances into the fabricated scaffolds to mimic the native cellular microenvironment is another similar method. Based on several research results, incorporation of electroactive materials leads to enhancement in tissue formation, such as increased differentiation and alignment while electrical stimuli are applied.^{41,140,141}

Materials with the ability to promote myoblast proliferation and myogenic differentiation are good candidates in skeletal muscle tissue engineering. Dong et al. synthesized an elastic conductive poly(ethylene glycol)-*co*-poly(glycerol sebacate) (PEGS) grafted aniline pentamer (AP) copolymer that promoted myotube formation by differentiating C2C12 mouse myoblast cells. Based on their results, by adjusting the AP and PEG content, the fabricated film revealed suitable surface hydrophilicity for cell attachment. Moreover, those films possessed tunable conductivity and mechanical properties that were controlled by a change in the content of AP. The maximum conductivity of the films was 1.84×10^{-4} S/cm (which falls within the range of cardiac muscle tissue conductivity $0.005 < 0.0184 < 0.16$ S/m).¹⁰ Their findings indicated that PEGS-AP films promoted the proliferation and myogenic differentiation of C2C12 cells.¹⁴²

In another study, Jo et al. made a highly flexible nanofibrous scaffold from polycarbonate diol and isosorbide ($C_6H_{10}O_4$)-based polyurethane and hydrophilic nano-GO. They found that GO incorporation increased the elasticity, hydrophilicity, and stress relaxation capacity of the nanofibrous scaffolds. The polyurethane-GO nanofibers enhanced the initial adhesion and spreading of C2C12 myoblast cells, and furthered their proliferation. Additionally, the polyurethane-GO scaffolds significantly upregulated the levels of

myogenic mRNA and myosin heavy chain expression. In dynamic force conditions, the C2C12 cells showed significantly higher myogenic differentiation markers at both protein and gene levels and promoted aligned myotubular formation. The maximum conductivity of the scaffold was 1 S/m.¹⁴³

Myotubes should be arranged linearly to mimic the native structure of muscle that is organized in an extremely linear manner, without branched bundles *in vivo*. This organization is partly interposed through the biological and physical attributes of the ECM. The ECM structure of skeletal muscle consists of a protein NF network, which has been repeated *ex vivo*, resulting in the linear orientation of differentiated initial skeletal muscle cells grown on microstructured conductive polymer platforms. This efficacy is achievable at the nanoscale by biodegradable nanofibers, showing that nano-designed scaffolds are able to control the orientation of such muscle fibers. The capability to restrain myoblast expansion into orientated myotubes is vital for efficient muscle engineering.¹⁴⁴ Conductive scaffolds used for muscular tissue engineering are listed in Table 5.

Concluding Remarks and Future Perspective

Nowadays, there is an unmet need for the development of tissue-engineered electroconductive constructs that can recapitulate the physicochemical, structural, functional, and biological properties of different native organs. Undoubtedly, conventional conductive materials exhibit certain limitations for improving the structural and functional integration between tissue-engineered scaffolds and the specific tissue target that needs to be regenerated. Fortunately, nevertheless, the emergence of nanotechnology in medicine (nanomedicine) has set high expectations for tremendous progress in addressing the complexities and difficulties in medicine and biological science due to the close relationship between biological systems and nanoscale features. Therefore, the development of novel and advanced nanobiomaterials would allow us to design nanofeatured systems that can be functional and translatable in real-life medicine, particularly in the field of regenerative medicine. Among the tissues and organs in the human body, some of them are more complicated, such as electrically conductive tissues. Therefore, the introduction and integration of conductive nanobiomaterials within natural polymeric materials that can mimic the ECM, is of great importance for finding solutions to recapitulate the structural and electrically conductive properties of native tissues such as the myocardium, skeletal muscle, nerve, and bone tissues.

Despite all the efforts in this field and with all the extensive research that has been done during the last decade on the development of electroconductive scaffolds for regenerative medicine, there are only a few examples of conductive polymers supported by clinical trials which becomes even less when considering conductive biodegradable nanobiomaterials that can support the strong contractile properties of native tissues along with suitable biodegradability and biocompatibility properties. As is well known, much of the research to date has shown that the physiological and structural characteristics of these conductive nanobiomaterials may change postimplantation and, thus, end in undesired toxicity, immune activation, or aggregation.^{37–39} Such unpredicted

changes in physiological characteristics of conductive NMs can add much more complexity to the immune system and inflammatory responses to the host body, which subsequently may lead to very adverse and dramatic effects. Therefore, it is not unrealistic to see why it has been so difficult for scientists to create U.S. Food and Drug Administration (FDA)-approved electroconductive biodegradable and biocompatible materials. This is also why some naturally conductive polymers (such as PLGA, PANI, PEDOT:PSS [polystyrenesulfonate], etc.), which do not exactly mimic natural tissue conductivity, remain the gold standard in the regenerative medicine field.

Therefore, we believe that the future biomaterials for tissue regeneration should be more focused toward designing, creating, and engineering electrically conductive, biodegradable and biocompatible materials to provide enhanced conductivity to further improve damaged tissue regeneration, while making sure that there would be no undesired side effects upon implantation in the body. As an example, as it is well known, one of the major problems associated with conductive polymers is their very slow (if any) *in vivo* degradation rate, which makes them inappropriate candidates for tissue engineering (such tissues constantly remodel) *in vivo* use due to their constant risk of inflammation. But one can increase the biodegradability of these conductive polymers by modifying the polymer itself, for instance, by introducing more hydrophilic cues, or through the addition of ionizable or hydrolyzable groups to their backbone, to make them biodegradably appropriate candidates for tissue regeneration purposes.^{41,162} To overcome the risk of inflammation in tissue regeneration processes, a pulsed electromagnetic field can be used as an emerging innovative treatment for the regulation of inflammation while significantly promoting tissue regeneration.¹⁶³

To overcome the slow degradation rate of these naturally conductive polymers, mixing with other biodegradable polymers would also be another strategy to alleviate this shortcoming; however, this never solves the degradability problem of a conductive polymer, and still, it might take a long time for natural body mechanisms to degrade a conductive polymer usually due to their highly stable carbon ring structures. One of the other challenges associated with these conductive polymers is optimization of conductivity. One of the approaches to tackle increasing the conductivity of natural conductive polymers (e.g., some of these polymers have inherently low conductivity which is not adequate to mimic the electrical conductivity of the native tissue), is to pay attention to the shape and architecture (such as star-shape, tetrapod, branched, etc.) of the synthesized polymer scaffold, which can be achieved during the design and synthesis process.¹⁶² However, we would emphasize that there are always complexities, complications, and contradictions in the optimization of these polymers for a specific tissue engineering application since one might lose or diminish a desirable characteristic in the way of improving other characteristics.

Among the tissue engineering and regenerative medicine community, naturally conductive polymers have yet remained as the gold standard for tissue regeneration (such as PLGA) because they are versatile; have tunable physicochemical, structural, and biological properties; are easily functionalized; can form different types of conductive scaffolds (as pristine, composite, hybrid, hydrogel, electrospun);

TABLE 5. NANOENGINEERED ELECTROCONDUCTIVE SCAFFOLDS FOR TENDON/SKELETAL MUSCLE TISSUE REGENERATION

Type of conductive scaffold	Composition	Fabrication technique	Measurement device	Cellular type	Properties	Ref.
Nanofibrous	Gelatin-PANI doped with CSA	Electrospinning	Four point probe measurements	Mouse C2C12 myoblast	Enhance myotube contractibility, DHPR colocalization, RyR, expression of genes correlated to the E-C coupling apparatus, calcium transients. The maximum conductivity was 4.2×10^{-3} S/cm.	145
Nanofibrous	PANI/PAN	Electrospinning	—	Mouse fibroblast cells and mesenchymal stem cells	Support cell growth and proliferation, promote hMSCs differentiation into muscle-like cells (gene expression and immunocytochemistry).	146
Nanofibrous	PANI/PAN	Electrospinning	—	Mouse satellite cells	Lower cell proliferation and highest value of differentiation. The maximum conductivity was 38.58 ± 0.09 μ S/cm.	147
Nanofibrous	PANI/Chitosan grafted aniline tetramer	Electrospinning	Cyclic voltammetry	C2C12 myoblasts and dog chondrocyte cells	Noncytotoxicity of products and improve the cell adhesion and proliferation of C2C12 myoblasts.	148
Nanofibrous	PANI and PCL	Electrospinning	Four-point probe measurements	C2C12 myoblasts	Guide myoblast orientation and promote myotube formation. Enhance myotube maturation. The maximum conductivity was 63.6 ± 6.6 mS/cm.	149
Nanofibrous	PANI and PCL	Electrospinning	Cyclic voltammetry	C2C12 myoblasts	MHC expression, formation of multinucleate myotube, the expression of differentiation-specific genes (myogenin, troponin-T, MHC).	150
Nanofibrous	PANI/Tetraaniline-poly lactide	Thermally-induced phase separation	Cyclic voltammetry	C2C12 myoblasts	Nonotoxicity, enhance the adhesion and proliferation of the C2C12 myoblast cells, significantly improve the cell proliferation of C2C12 myoblasts.	151
Nanofibrous	PAN/PANI-CSA/GO	Electrospinning	Four-point probe measurements	Mouse satellite cells	Enhanced conductivity, relative higher stiffness of the PAN/PANI-CSA/G nanofibers. The maximum conductivity was 159.69 ± 0.06 μ S/cm.	152
Nanofibrous	SF/PASA	Electrospinning	Four-point probe measurements	L929 and C2C12 cells	Enhanced the myogenic differentiation of C2C12 cells. The maximum conductivity was 10^{-2} S/m.	153
Nanofibrous	PCL/PPy	Electrospinning	DC voltage	C2C12 myoblasts	Promoted myoblast differentiation to a greater extent than scaffolds made of PCL. The maximum conductivity was 1.1 mS/cm.	154
Nanofibrous	Polycaprolactone/polyaniline	Electrospinning	Four-point probe measurements	hADSCs	Increased conductivity with the inclusion of polyaniline. Scaffolds with 0.1% wt. polyaniline showed suitable compressive strength and conductivity for bone tissue engineering applications. The maximum conductivity was 2.46×10^{-4} S/cm.	155

(continued)

TABLE 5. (CONTINUED)

Type of conductive scaffold	Composition	Fabrication technique	Measurement device	Cellular type	Properties	Ref.
Nanofibrous	Polyurethane/GO	Electrospinning	—	C2C12 myoblasts	Upregulated the myogenic mRNA levels and myosin heavy chain expression. Expressed significantly higher myogenic cell differentiation markers at both gene and protein levels and more aligned myotubular formation.	143
Thin Films	ACAT/PUU	Mixing	Cyclic voltammetry	C2C12 myoblasts	The maximum conductivity was 1 S/cm. Promote cell proliferation, myotube formation (mRNA and protein level).	156
Films	AP/PEGS	Mixing	True RMS OLED Multimeter	C2C12 myoblasts	The maximum conductivity was 10^{-6} S/cm. Promote cell proliferation, myotube formation (mRNA and protein level).	142
Films	Polyurethane/(1S)-(+)–10-camphorsulfonic acid	Solvent evaporation	Cyclic voltammetry	Mouse 3T3 fibroblasts	The maximum conductivity was 1.84×10^{-4} S/cm. Good elasticity, electrical stability, and biocompatibility.	157
Hydrogels	GG/PPy	Chemical oxidative polymerization	Four-point probe measurements	929 and C2C12 myoblast cells	The maximum conductivity was 7.3×10^{-5} S/cm. Nontoxic for L929 cells. L929 and C2C12 myoblast cells were able to adhere and spread within hydrogels.	158
Hydrogels	Dextran-graft-aniline tetramer-graft-4-formylbenzoic acid and <i>N</i> -carboxyethyl chitosan	Green approach by the Michael addition reaction	Cyclic voltammetry	C2C12 myoblasts, HUVEC	The maximum conductivity was 2.05×10^{-4} S/cm. Released the C2C12 myoblast cells with a linear-like profile. Adequate <i>in vivo</i> injectability and <i>in vivo</i> degradability of hydrogels.	159
Hydrogels	MnO ₂ /polyaniline/MWCNTs/r-GOx	Mixing	Cyclic voltammetry	—	The maximum conductivity was 3.4×10^{-4} mS/cm. Outstanding ion transportation efficiency, mechanical properties, and electrochemical properties. The maximum conductivity was 0.182 mS/cm.	160
Hydrogels	GelMA-alginate bioinks	Bioprinting	Two-channel stimulator	Mouse-derived C2C12 myoblast cells	Improved metabolic activity of cells in GelMA bioinks by addition of oxygen-generating particles to the bioinks.	161

ACAT, aniline trimer; CSA, camphorsulfonic acid; E–C, excitation–contraction; DHPR, dihydropyridine receptor; GG, gellan gum; hADSCs, human adipose-derived stem cells; HUVEC, human umbilical vein endothelial cells; MHC, myosin heavy chain; MnO₂, manganese dioxide; PASA, poly(aniline-co-*N*-(4-sulfophenyl) aniline); PEGS, poly(ethylene glycol)-co-poly(glycerol sebacate); PUU, polyurethane-urea; rGO, reduced graphene oxide; RyR, ryanodine receptor.

and also can be optimized to be biodegradable and biocompatible for a specific application. Therefore, it is no wonder that these smart conductive polymers are receiving increasing attention between scientists for various biomedical applications, particularly tissue engineering and regenerative medicine, drug delivery systems, and biosensors. Overall, and in particular, biodegradable and electroconductive polymers continue to have the potential to revolutionize the field of electrically conductive tissue regeneration, answers for which we are still awaiting.

The development of a clinically appropriate electroconductive scaffold than can mimic the physicochemical, functional, and structural properties of a specific tissue/organ for regenerative purposes is a huge challenge in the field. Despite tremendous enhancement *in vitro* regarding the applicability of the electroconductive nanoengineered scaffolds, the successful translation of these nanosystems face obvious challenges when applied *in vivo*, as it is inherent to other NMs. While interest in the use of conductive nanoadditives and their incorporation into polymeric scaffolds has surged over the past decade, and there are numerous reports on the development of electroconductive nanobiomaterial, most of them still need further evaluations in clinical trials. Therefore, this could be another reason why we strongly believe naturally derived electroconductive polymers have still remained as the most trusted source of tissue-engineered scaffolds for regenerative applications.

Another future perspective in terms of overcoming the safety and *in vivo* toxicity challenges associated with the incorporation of nanoscale additives into bioengineered scaffolds (such as AuNPs) to grant them appropriate conductivity, is the synthesis of these NMs. Green nanotechnology has appeared as a novel approach to tackle some of the most concerning problems related to the use of NMs, especially in terms of synthesis and functionalization of NMs that are going to be used in biomedical applications. In this regard, the implementation of green nanotechnology practices within nanoparticle synthesis is allowing for a quick, efficient, cost-effective, and environmentally friendly generation of different nanosystems without compromising their biomedical activity.¹⁶⁴ As a consequence, great efforts have been made to establish green nanotechnology approaches in the field: from the use of bacteria or fungi as raw materials, to the employment of plant extracts or waste materials.^{165,166} Therefore, these green NMs have been used in different applications in the biomedical field.^{98,167} In terms of electroconductive NMs, not many examples have been recently released to literature, however, efforts toward this end have shown that the use of green practices can allow for a sustainable production of such NMs and their successful application within tissue engineering and regenerative medicine. Advantages in this regard include enhanced biocompatibility, reduced localized cytotoxicity, and a better integration of the targeted tissue within the nanoplatform, all of which are extremely desired for any application involving the migration, growth, establishment, and proliferation of different cell types in regenerative approaches.^{168,169}

Authors' Contributions

E.M. outlined the article. E.M., D.M.C., K.K., A.T., and P.S. wrote the article. E.M., D.M.C., K.K., A.T. prepared the

figures and tables. E.M., D.M.C., and T.J.W. revised the article. E.M. performed the corrections and finalized the article. T.J.W. supervised the work.

Author Disclosure Statement

No competing financial interests exist.

Funding Information

The authors would like to acknowledge Northeastern University for funding the authors.

References

1. Liu Y, Lim J, Teoh S-H. Development of clinically relevant scaffolds for vascularised bone tissue engineering. *Biotechnol Adv* 2013;31:688–705.
2. Hosoyama K, Ahumada M, Goel K, et al. Electroconductive materials as biomimetic platforms for tissue regeneration. *Biotechnol Adv* 2019;37:444–458.
3. Fennelly C, Soker S. Bioelectric properties of myogenic progenitor cells. *Bioelectricity* 2019;1:35–45.
4. Saberi A, Jabbari F, Zarrintaj P, et al. Electrically conductive materials: opportunities and challenges in tissue engineering. *Biomolecules* 2019;9:448.
5. Bassett CAL, Becker RO. Generation of electric potentials by bone in response to mechanical stress. *Science* 1962;137:1063–1064.
6. Mostafavi E, Soltantabar P, Webster TJ. Nanotechnology and picotechnology: A new arena for translational medicine. *Biomater Transl Med* 2019;1:191–212.
7. Kalantari K, Mostafavi E, Afifi AM, et al. Wound dressings functionalized with silver nanoparticles: Promises and pitfalls. *Nanoscale* 2020;12:2268–2291.
8. Rahmani Del Bakhshayesh A, Mostafavi E, Alizadeh E, et al. Fabrication of three-dimensional scaffolds based on nano-biomimetic collagen hybrid constructs for skin tissue engineering. *ACS Omega* 2018;3:8605–8611.
9. Zarrintaj P, Manouchehri S, Ahmadi Z, et al. Agarose-based biomaterials for tissue engineering. *Carbohydr Polym* 2018;187:66–84.
10. Stout DA, Yoo J, Santiago-Miranda AN, et al. Mechanisms of greater cardiomyocyte functions on conductive nanoengineered composites for cardiovascular application. *Int J Nanomedicine* 2012;7:5653.
11. Tay A. Materials meet bioelectrical and-mechanical demands of the heart. *MRS Bull* 2018;43:566–567.
12. Benjamin EJ, Muntner P, Bittencourt MS. Heart disease and stroke statistics-2019 update: A report from the American Heart Association. *Circulation* 2019;139:e56–e528.
13. Adadi N, Yadid M, Gal I, et al. Electrospun fibrous PVDF-TrFe scaffolds for cardiac tissue engineering, differentiation, and maturation. *Adv Mater Technol* 2020;5:1900820.
14. Mahmoudi M, Yu M, Serpooshan V, et al. Multiscale technologies for treatment of ischemic cardiomyopathy. *Nat Nanotechnol* 2017;12:845.
15. Yanamandala M, Zhu W, Garry DJ, et al. Overcoming the roadblocks to cardiac cell therapy using tissue engineering. *J Am Coll Cardiol* 2017;70:766–775.
16. Kitsara M, Agbulut O, Kontziampasis D, et al. Fibers for hearts: A critical review on electrospinning for cardiac tissue engineering. *Acta Biomater* 2017;48:20–40.

17. Nafee T, Gibson CM, Yee MK, et al. Betrixaban for first-line venous thromboembolism prevention in acute medically ill patients with risk factors for venous thromboembolism. *Expert Rev Cardiovasc Ther* 2018; 16:845–855.
18. Wang L, Wu Y, Hu T, et al. Electrospun conductive nanofibrous scaffolds for engineering cardiac tissue and 3D bioactuators. *Acta Biomater* 2017;59:68–81.
19. Boffito M, Sartori S, Ciardelli G. Polymeric scaffolds for cardiac tissue engineering: Requirements and fabrication technologies. *Polym Int* 2014;63:2–11.
20. Capulli A, MacQueen L, Sheehy SP, et al. Fibrous scaffolds for building hearts and heart parts. *Adv Drug Deliv Rev* 2016;96:83–102.
21. Kaiser NJ, Coulombe KL. Physiologically inspired cardiac scaffolds for tailored in vivo function and heart regeneration. *Biomed Mater* 2015;10:034003.
22. McLaughlin S, Podrebarac J, Ruel M, et al. Nano-engineered biomaterials for tissue regeneration: What has been achieved so far? *Front Mater* 2016;3:27.
23. Dvir T, Timko BP, Brigham MD, et al. Nanowired three-dimensional cardiac patches. *Nat Nanotechnol* 2011;6:720.
24. Wei K, Serpooshan V, Hurtado C, et al. Epicardial FSTL1 reconstitution regenerates the adult mammalian heart. *Nature* 2015;525:479.
25. Fleischer S, Feiner R, Dvir T. Cardiac tissue engineering: From matrix design to the engineering of bionic hearts. *Regen Med* 2017;12:275–284.
26. Khan M, Xu Y, Hua S, et al. Evaluation of changes in morphology and function of human induced pluripotent stem cell derived cardiomyocytes (hiPSC-CMs) cultured on an aligned-nanofiber cardiac patch. *PLoS One* 2015;10: e0126338.
27. Bursac N, Loo Y, Leong K, et al. Novel anisotropic engineered cardiac tissues: Studies of electrical propagation. *Biochem Biophys Res Commun* 2007;361:847–853.
28. Liang S, Zhang Y, Wang H, et al. Paintable and rapidly bondable conductive hydrogels as therapeutic cardiac patches. *Adv Mater* 2018;30:1704235.
29. Navaei A, Eliato KR, Ros R, et al. The influence of electrically conductive and non-conductive nanocomposite scaffolds on the maturation and excitability of engineered cardiac tissues. *Biomater Sci* 2019;7:585–595.
30. Goenka S, Sant V, Sant S. Graphene-based nanomaterials for drug delivery and tissue engineering. *J Control Release* 2014;173:75–88.
31. Amani H, Mostafavi E, Arzaghi H, et al. Three-dimensional graphene foams: Synthesis, properties, biocompatibility, biodegradability, and applications in tissue engineering. *ACS Biomater Sci Eng* 2018;5:193–214.
32. Min JH, Patel M, Koh W-G. Incorporation of conductive materials into hydrogels for tissue engineering applications. *Polymers* 2018;10:1078.
33. Shin SR, Li Y-C, Jang HL, et al. Graphene-based materials for tissue engineering. *Adv Drug Deliv Rev* 2016; 105:255–274.
34. Lakshmanan R, Krishnan UM, Sethuraman S. Living cardiac patch: The elixir for cardiac regeneration. *Expert Opin Biol Ther* 2012;12:1623–1640.
35. Kiew SF, Kiew LV, Lee HB, et al. Assessing biocompatibility of graphene oxide-based nanocarriers: A review. *J Control Release* 2016;226:217–228.
36. Malki M, Fleischer S, Shapira A, et al. Gold nanorod-based engineered cardiac patch for suture-free engraftment by near IR. *Nano Lett* 2018;18:4069–4073.
37. Hajipour MJ, Mehrani M, Abbasi SH, et al. Nanoscale technologies for prevention and treatment of heart failure: Challenges and opportunities. *Chem Rev* 2019;119:11352–11390.
38. Kreyling WG, Abdelmonem AM, Ali Z, et al. In vivo integrity of polymer-coated gold nanoparticles. *Nat Nanotechnol* 2015;10:619.
39. Deng ZJ, Liang M, Monteiro M, et al. Nanoparticle-induced unfolding of fibrinogen promotes Mac-1 receptor activation and inflammation. *Nat Nanotechnol* 2011;6: 39–44.
40. Ahmadvani L, Mostafavi E, Ghasemali S, et al. Development and characterization of a novel conductive polyaniline-g-polystyrene/Fe₃O₄ nanocomposite for the treatment of cancer. *Artif Cells Nanomed Biotechnol* 2019;47:873–881.
41. Balint R, Cassidy NJ, Cartmell SH. Conductive polymers: Towards a smart biomaterial for tissue engineering. *Acta Biomater* 2014;10:2341–2353.
42. Guo B, Ma PX. Conducting polymers for tissue engineering. *Biomacromolecules* 2018;19:1764–1782.
43. Xu C, Huang Y, Yezpe G, et al. Development of dopant-free conductive bioelastomers. *Sci Rep* 2016;6:1–13.
44. Wang L, Jiang J, Hua W, et al. Mussel-inspired conductive cryogel as cardiac tissue patch to repair myocardial infarction by migration of conductive nanoparticles. *Adv Funct Mater* 2016;26:4293–4305.
45. Shin SR, Shin C, Memic A, et al. Aligned carbon nanotube-based flexible gel substrates for engineering biohybrid tissue actuators. *Adv Funct Mater* 2015;25:4486–4495.
46. Noor N, Shapira A, Edri R, et al. 3D printing of personalized thick and perfusable cardiac patches and hearts. *Adv Sci* 2019;6:1900344.
47. Montgomery M, Ahadian S, Huyer LD, et al. Flexible shape-memory scaffold for minimally invasive delivery of functional tissues. *Nat Mater* 2017;16:1038–1046.
48. Wu Y, Chen YX, Yan J, et al. Fabrication of conductive gelatin methacrylate–polyaniline hydrogels. *Acta Biomater* 2016;33:122–130.
49. Spencer AR, Primbetova A, Koppes AN, et al. Electroconductive gelatin methacryloyl-PEDOT: PSS composite hydrogels: Design, synthesis, and properties. *ACS Biomater Sci Eng* 2018;4:1558–1567.
50. Shin SR, Zihlmann C, Akbari M, et al. Reduced graphene oxide-gelMA hybrid hydrogels as scaffolds for cardiac tissue engineering. *Small* 2016;12:3677–3689.
51. Cabiati M, Vozzi F, Gemma F, et al. Cardiac tissue regeneration: A preliminary study on carbon-based nanotubes gelatin scaffold. *J Biomed Mater Res B Appl Biomater* 2018;106:2750–2762.
52. Dong R, Zhao X, Guo B, et al. Self-healing conductive injectable hydrogels with antibacterial activity as cell delivery carrier for cardiac cell therapy. *ACS Appl Mater Interfaces* 2016;8:17138–17150.
53. Yu H, Zhao H, Huang C, et al. Mechanically and electrically enhanced CNT–collagen hydrogels as potential scaffolds for engineered cardiac constructs. *ACS Biomater Sci Eng* 2017;3:3017–3021.
54. Roshanbinfar K, Hilborn J, Varghese OP, et al. Injectable and thermoresponsive pericardial matrix derived conductive scaffold for cardiac tissue engineering. *RSC Adv* 2017;7: 31980–31988.

55. Baheiraei N, Yeganeh H, Ai J, et al. Preparation of a porous conductive scaffold from aniline pentamer-modified polyurethane/PCL blend for cardiac tissue engineering. *J Biomed Mater Res A* 2015;103:3179–3187.
56. Walker BW, Lara RP, Yu CH, et al. Engineering a naturally-derived adhesive and conductive cardiopatch. *Biomaterials* 2019;207:89–101.
57. Gelmi A, Cieslar-Pobuda A, de Muinck E, et al. Direct mechanical stimulation of stem cells: A beating electro-mechanically active scaffold for cardiac tissue engineering. *Adv Healthc Mater* 2016;5:1471–1480.
58. Wan AM-D, Inal S, Williams T, et al. 3D conducting polymer platforms for electrical control of protein conformation and cellular functions. *J Mater Chem B* 2015;3:5040–5048.
59. Zanzanjadeh Ezazi N, Ajdary R, Correia A, et al. Fabrication and characterization of drug-loaded conductive poly (glycerol sebacate)/nanoparticle-based composite patch for myocardial infarction applications. *ACS Appl Mater Interfaces* 2020;12:6899–6909.
60. Ahadian S, Huyer LD, Estili M, et al. Moldable elastomeric polyester-carbon nanotube scaffolds for cardiac tissue engineering. *Acta Biomater* 2017;52:81–91.
61. Wu Y, Wang L, Guo B, et al. Interwoven aligned conductive nanofiber yarn/hydrogel composite scaffolds for engineered 3D cardiac anisotropy. *ACS Nano* 2017;11:5646–5659.
62. Sun H, Lü S, Jiang X-X, et al. Carbon nanotubes enhance intercalated disc assembly in cardiac myocytes via the β 1-integrin-mediated signaling pathway. *Biomaterials* 2015;55:84–95.
63. Puckert C, Gelmi A, Ljunggren M, et al. Optimisation of conductive polymer biomaterials for cardiac progenitor cells. *RSC Adv* 2016;6:62270–62277.
64. Ho CMB, Mishra A, Lin PTP, et al. 3D printed polycaprolactone carbon nanotube composite scaffolds for cardiac tissue engineering. *Macromol Biosci* 2017;17:1600250.
65. Ceña V, Játiva P. Nanoparticle crossing of blood–brain barrier: A road to new therapeutic approaches to central nervous system diseases. *Nanomedicine (Lond)* 2018;13:1513–1516.
66. Seven ES, Zhou Y, Seven YB, et al. Crossing blood-brain barrier with carbon quantum dots. *FASEB J* 2019;33(1 Suppl):785.8–785.8.
67. Zhou Y, Zhao H, Ma D, et al. Harnessing the properties of colloidal quantum dots in luminescent solar concentrators. *Chem Soc Rev* 2018;47:5866–5890.
68. Soltantabar P, Calubaquib EL, Mostafavi E, et al. Enhancement of loading efficiency by co-loading of doxorubicin and quercetin in thermoresponsive polymeric micelles. *Biomacromolecules* 2020;21:1427–1436.
69. Ledesma HA, Li X, Carvalho-de-Souza JL, et al. An atlas of nano-enabled neural interfaces. *Nat Nanotechnol* 2019;14:645–657.
70. Kang YJ, Cutler EG, Cho H. Therapeutic nanoplatfoms and delivery strategies for neurological disorders. *Nano Converg* 2018;5:35.
71. Koffler J, Zhu W, Qu X, et al. Biomimetic 3D-printed scaffolds for spinal cord injury repair. *Nat Med* 2019;25:263–269.
72. Mohs AM, Provenzale JM. Applications of nanotechnology to imaging and therapy of brain tumors. *Neuroimaging Clin N Am* 2010;20:283–292.
73. Meola A, Rao J, Chaudhary N, et al. Gold nanoparticles for brain tumor imaging: A systematic review. *Front Neurol* 2018;9:328.
74. Amani H, Mostafavi E, Alebouyeh MR, et al. Would colloidal gold nanocarriers present an effective diagnosis or treatment for ischemic stroke? *Int J Nanomedicine* 2019;14:8013.
75. Cheng Y, Meyers JD, Agnes RS, et al. Addressing brain tumors with targeted gold nanoparticles: A new gold standard for hydrophobic drug delivery? *Small* 2011;7:2301–2306.
76. Pampaloni NP, Giugliano M, Scaini D, et al. Advances in nano neuroscience: From nanomaterials to nanotools. *Front Neurosci* 2019;12:953.
77. Monaco AM, Giugliano M. Carbon-based smart nanomaterials in biomedicine and neuroengineering. *Beilstein J Nanotechnol* 2014;5:1849–1863.
78. Kaushik A, Jayant RD, Nair M. Nanomedicine for neuroHIV/AIDS management. *Nanomedicine (Lond)* 2018;13:669–673.
79. Hubert V, Dumot C, Ong E, et al. MRI coupled with clinically-applicable iron oxide nanoparticles reveals choroid plexus involvement in a murine model of neuroinflammation. *Sci Rep* 2019;9:10046.
80. Kuo Y-C, Cheng S-J. Brain targeted delivery of carmustine using solid lipid nanoparticles modified with tamoxifen and lactoferrin for antitumor proliferation. *Int J Pharm* 2016;499:10–19.
81. Liu X, Miller AL, Park S, et al. Functionalized carbon nanotube and graphene oxide embedded electrically conductive hydrogel synergistically stimulates nerve cell differentiation. *ACS Appl Mater Interfaces* 2017;9:14677–14690.
82. Sanjairaj V, Kannan S, Cao T, et al. 3D-Printed PCL/PPy conductive scaffolds as three-dimensional porous nerve guide conduits (NGCs) for peripheral nerve injury repair. *Front Bioeng Biotechnol* 2019;7:266.
83. Cheng Y, Xu Y, Qian Y, et al. 3D structured self-powered PVDF/PCL scaffolds for peripheral nerve regeneration. *Nano Energy* 2020;69:104411.
84. Nezakati T, Tan A, Lim J, et al. Ultra-low percolation threshold POSS-PCL/graphene electrically conductive polymer: Neural tissue engineering nanocomposites for neurosurgery. *Mater Sci Eng C* 2019;104:109915.
85. Aval NA, Emadi R, Valiani A, et al. Nano-featured poly (lactide-co-glycolide)-graphene microribbons as a promising substrate for nerve tissue engineering. *Compos Part B Eng* 2019;173:106863.
86. Pillai MM, Kumar GS, Houshyar S, et al. Effect of nanocomposite coating and biomolecule functionalization on silk fibroin based conducting 3D braided scaffolds for peripheral nerve tissue engineering. *Nanomed Nanotechnol Biol Med* 2020;24:102131.
87. Liu Q, Liu G, Liu X, et al. Synthesis of an electrospun PHA/RGO/Au scaffold for peripheral nerve regeneration: An in vitro study. *Appl Nanosci* 2020;10:687–694.
88. Abzan N, Kharaziha M, Labbaf S. Development of three-dimensional piezoelectric polyvinylidene fluoride-graphene oxide scaffold by non-solvent induced phase separation method for nerve tissue engineering. *Mater Design* 2019;167:107636.
89. Eatemadi A, Daraee H, Karimkhanloo H, et al. Carbon nanotubes: Properties, synthesis, purification, and medical applications. *Nanoscale Res Lett* 2014;9:393.

90. Malarkey EB, Parpura V. Carbon nanotubes in neuroscience. *Acta Neurochir Suppl* 2010;106:337–341.
91. Mattson MP, Haddon RC, Rao AM. Molecular functionalization of carbon nanotubes and use as substrates for neuronal growth. *J Mol Neurosci* 2000;14:175–182.
92. Lee C-S, Kim SK, Kim M. Ion-sensitive field-effect transistor for biological sensing. *Sensors* 2009;9:7111–7131.
93. Dale N, Hatz S, Tian F, et al. Listening to the brain: Microelectrode biosensors for neurochemicals. *Trends Biotechnol* 2005;23:420–428.
94. Balasundaram G, Webster TJ. Nanotechnology and biomaterials for orthopedic medical applications. *Nanomedicine (Lond)* 2006;1:169–176.
95. Gong T, Xie J, Liao J, et al. Nanomaterials and bone regeneration. *Bone Res* 2015;3:15029.
96. Ramos R, Zhang K, Quinn D, et al. Measuring changes in electrical impedance during cell-mediated mineralization. *Bioelectricity* 2019;1:73–84.
97. Cheng H, Chawla A, Yang Y, et al. Development of nanomaterials for bone-targeted drug delivery. *Drug Discov Today* 2017;22:1336–1350.
98. Medina-Cruz D, Mostafavi E, Vernet-Crua A, et al. Green nanotechnology-based drug delivery systems for osteogenic disorders. *Expert Opin Drug Deliv* 2020;17:341–356.
99. Balmer TW, Vesztegom S, Broekmann P, et al. Characterization of the electrical conductivity of bone and its correlation to osseous structure. *Sci Rep* 2018;8:8601.
100. Haba Y, Wurm A, Köckerling M, et al. Characterization of human cancellous and subchondral bone with respect to electro physical properties and bone mineral density by means of impedance spectroscopy. *Med Eng Phys* 2017;45:34–41.
101. Chen C, Yu Y, Li K, et al. Facile approach to the fabrication of 3D electroconductive nanofibers with controlled size and conductivity templated by bacterial cellulose. *Cellulose* 2015;22:3929–3939.
102. Isaacson BM, Bloebaum RD. Bone bioelectricity: What have we learned in the past 160 years? *J Biomed Mater Res A* 2010;95:1270–1279.
103. Tandon B, Blaker JJ, Cartmell SH. Piezoelectric materials as stimulatory biomedical materials and scaffolds for bone repair. *Acta Biomater* 2018;73:1–20.
104. Tang Y, Wu C, Wu Z, et al. Fabrication and in vitro biological properties of piezoelectric bioceramics for bone regeneration. *Sci Rep* 2017;7:43360.
105. Bao S, Liang G, Tjong SC. Effect of mechanical stretching on electrical conductivity and positive temperature coefficient characteristics of poly (vinylidene fluoride)/carbon nanofiber composites prepared by non-solvent precipitation. *Carbon* 2011;49:1758–1768.
106. Li Y, Ge X, Wang L, et al. Dielectric relaxation behavior of PVDF composites with nanofillers of different conductive nature. *Curr Nanosci* 2013;9:679–685.
107. Wright Z, Arnold A, Holt B, et al. Functional graphenic materials, graphene oxide, and graphene as scaffolds for bone regeneration. *Regen Eng Transl Med* 2019;5:190–209.
108. Samadian H, Mobasheri H, Hasanpour S, et al. Electroconductive carbon nanofibers as the promising interfacial biomaterials for bone tissue engineering. *J Mol Liquids* 2020;298:112021.
109. Chen J, Yu M, Guo B, et al. Conductive nanofibrous composite scaffolds based on in-situ formed polyaniline nanoparticle and polylactide for bone regeneration. *J Colloid Interface Sci* 2018;514:517–527.
110. Khorshidi S, Karkhaneh A. Hydrogel/fiber conductive scaffold for bone tissue engineering. *J Biomed Mater Res A* 2018;106:718–724.
111. Castro AG, Diba M, Kersten M, et al. Development of a PCL-silica nanoparticles composite membrane for guided bone regeneration. *Mater Sci Eng C* 2018;85:154–161.
112. Hu Y, Ke L, Chen H, et al. Natural material-decorated mesoporous silica nanoparticle container for multifunctional membrane-controlled targeted drug delivery. *Int J Nanomed* 2017;12:8411.
113. Gao X, Lan J, Jia X, et al. Improving interfacial adhesion with epoxy matrix using hybridized carbon nanofibers containing calcium phosphate nanoparticles for bone repairing. *Mater Sci Eng C* 2016;61:174–179.
114. Feng Z, Li Y, Hao L, et al. Graphene-reinforced biodegradable resin composites for stereolithographic 3D printing of bone structure scaffolds. *J Nanomater* 2019;2019:13.
115. Miri AK, Mostafavi E, Khorsandi D, et al. Bioprinters for organs-on-chips. *Biofabrication* 2019;11:042002.
116. Huang Y, Deng H, Fan Y, et al. Conductive nanostructured Si biomaterials enhance osteogenesis through electrical stimulation. *Mater Sci Eng C* 2019;103:109748.
117. Holmes B, Fang X, Zarate A, et al. Enhanced human bone marrow mesenchymal stem cell chondrogenic differentiation in electrospun constructs with carbon nanomaterials. *Carbon* 2016;97:1–13.
118. Tan F, Liu J, Song K, et al. Effect of surface charge on osteoblastic proliferation and differentiation on a poly (ethylene glycol)-diacrylate hydrogel. *J Mater Sci* 2018;53:908–920.
119. Samadi A, Hasanzadeh R, Azdast T, et al. Piezoelectric performance of microcellular polypropylene foams fabricated using foam injection molding as a potential scaffold for bone tissue engineering. *J Macromol Sci B* 2020;59:376–389.
120. Polley C, Distler T, Detsch R, et al. 3D printing of piezoelectric barium titanate-hydroxyapatite scaffolds with interconnected porosity for bone tissue engineering. *Materials* 2020;13:1773.
121. Ehterami A, Kazemi M, Nazari B, et al. Fabrication and characterization of highly porous barium titanate based scaffold coated by Gel/HA nanocomposite with high piezoelectric coefficient for bone tissue engineering applications. *J Mech Behav Biomed Mater* 2018;79:195–202.
122. Zhang C, Wang X, Zhang E, et al. An epigenetic bioactive composite scaffold with well-aligned nanofibers for functional tendon tissue engineering. *Acta Biomater* 2018;66:141–156.
123. Rinoldi C, Fallahi A, Yazdi IK, et al. Mechanical and biochemical stimulation of 3d multilayered scaffolds for tendon tissue engineering. *ACS Biomater Sci Eng* 2019;5:2953–2964.
124. Longo UG, Lamberti A, Maffulli N, et al. Tendon augmentation grafts: A systematic review. *Br Med Bull* 2010;94:165.
125. Leong NL, Petrigliano FA, McAllister DR. Current tissue engineering strategies in anterior cruciate ligament reconstruction. *J Biomed Mater Res A* 2014;102:1614–1624.
126. Idaszek J, Kijeńska E, Łojkowski M, et al. How important are scaffolds and their surface properties in regenerative medicine. *Appl Surf Sci* 2016;388:762–774.

127. Serena E, Flaibani M, Carnio S, et al. Electrophysiologic stimulation improves myogenic potential of muscle precursor cells grown in a 3D collagen scaffold. *Neurol Res* 2008;30:207–214.
128. Nakayama KH, Shayan M, Huang NF. Engineering biomimetic materials for skeletal muscle repair and regeneration. *Adv Healthc Mater* 2019;8:1801168.
129. Kwee BJ, Mooney DJ. Biomaterials for skeletal muscle tissue engineering. *Curr Opin Biotechnol* 2017;47:16–22.
130. Chuang DC-C. Free tissue transfer for the treatment of facial paralysis. *Facial Plast Surg* 2008;24:194–203.
131. Palmieri B, Tremblay JP, Daniele L. Past, present and future of myoblast transplantation in the treatment of Duchenne muscular dystrophy. *Pediatr Transplant* 2010;14:813–819.
132. Capellato P, Escada AL, Popat KC, et al. Interaction between mesenchymal stem cells and Ti-30Ta alloy after surface treatment. *J Biomed Mater Res A* 2014;102:2147–2156.
133. Hiltunen M, Pelto J, Ellä V, et al. Uniform and electrically conductive biopolymer-doped polypyrrole coating for fibrous PLA. *J Biomed Mater Res B Appl Biomater* 2016;104:1721–1729.
134. Jin G, Li K. The electrically conductive scaffold as the skeleton of stem cell niche in regenerative medicine. *Mater Sci Eng C* 2014;45:671–681.
135. Collier JH, Camp JP, Hudson TW, et al. Synthesis and characterization of polypyrrole–hyaluronic acid composite biomaterials for tissue engineering applications. *J Biomed Mater Res* 2000;50:574–584.
136. Breukers R, Gilmore K, Kita M, et al. Creating conductive structures for cell growth: Growth and alignment of myogenic cell types on polythiophenes. *J Biomed Mater Res A* 2010;95:256–268.
137. Bach A, Beier J, Stern-Staeter J, et al. Skeletal muscle tissue engineering. *J Cell Mol Med* 2004;8:413–422.
138. Gilmore KJ, Kita M, Han Y, et al. Skeletal muscle cell proliferation and differentiation on polypyrrole substrates doped with extracellular matrix components. *Biomaterials* 2009;30:5292–5304.
139. Rodriguez BL, Larkin LM. Functional three-dimensional scaffolds for skeletal muscle tissue engineering. In: Deng Y, Kuiper J, eds. *Functional 3D Tissue Engineering Scaffolds*. Cambridge, UK: Woodhead Publishing, 2018: 279–304.
140. Sirivisoot S, Pareta R, Harrison BS. Protocol and cell responses in three-dimensional conductive collagen gel scaffolds with conductive polymer nanofibres for tissue regeneration. *Interface Focus* 2014;4:20130050.
141. Manchineella S, Thirivikraman G, Khanum KK, et al. Pigmented silk nanofibrous composite for skeletal muscle tissue engineering. *Adv Healthc Mater* 2016;5:1222–1232.
142. Dong R, Zhao X, Guo B, et al. Biocompatible elastic conductive films significantly enhanced myogenic differentiation of myoblast for skeletal muscle regeneration. *Biomacromolecules* 2017;18:2808–2819.
143. Jo SB, Erdenebileg U, Dashnyam K, et al. Nano-graphene oxide/polyurethane nanofibers: Mechanically flexible and myogenic stimulating matrix for skeletal tissue engineering. *J Tissue Eng* 2020;11:2041731419900424.
144. Quigley AF, Razal JM, Kita M, et al. Electrical stimulation of myoblast proliferation and differentiation on aligned nanostructured conductive polymer platforms. *Adv Healthc Mater* 2012;1:801–808.
145. Ostrovidov S, Ebrahimi M, Bae H, et al. Gelatin–polyaniline composite nanofibers enhanced excitation–contraction coupling system maturation in myotubes. *ACS Appl Mater Interfaces* 2017;9:42444–42458.
146. Mohamadali M, Irani S, Soleimani M, et al. PANi/PAN copolymer as scaffolds for the muscle cell-like differentiation of mesenchymal stem cells. *Polym Adv Technol* 2017;28:1078–1087.
147. Hosseinzadeh S, Mahmoudifard M, Mohamadyar-Toupkanlou F, et al. The nanofibrous PAN-PANi scaffold as an efficient substrate for skeletal muscle differentiation using satellite cells. *Bioprocess Biosyst Eng* 2016;39:1163–1172.
148. Ma X, Ge J, Li Y, et al. Nanofibrous electroactive scaffolds from a chitosan-grafted-aniline tetramer by electrospinning for tissue engineering. *RSC Adv* 2014;4:13652–13661.
149. Chen M-C, Sun Y-C, Chen Y-H. Electrically conductive nanofibers with highly oriented structures and their potential application in skeletal muscle tissue engineering. *Acta Biomater* 2013;9:5562–5572.
150. Ku SH, Lee SH, Park CB. Synergic effects of nanofiber alignment and electroactivity on myoblast differentiation. *Biomaterials* 2012;33:6098–6104.
151. Li L, Ge J, Wang L, et al. Electroactive nanofibrous biomimetic scaffolds by thermally induced phase separation. *J Mater Chem B* 2014;2:6119–6130.
152. Mahmoudifard M, Soleimani M, Hatamie S, et al. The different fate of satellite cells on conductive composite electrospun nanofibers with graphene and graphene oxide nanosheets. *Biomed Mater* 2016;11:025006.
153. Zhang M, Guo B. Electroactive 3D scaffolds based on silk fibroin and water-borne polyaniline for skeletal muscle tissue engineering. *Macromol Biosci* 2017;17:1700147.
154. Browe D, Freeman J. Optimizing C2C12 myoblast differentiation using polycaprolactone–polypyrrole copolymer scaffolds. *J Biomed Mater Res A* 2019;107:220–231.
155. Wibowo A, Vyas C, Cooper G, et al. 3D printing of polycaprolactone–polyaniline electroactive scaffolds for bone tissue engineering. *Materials* 2020;13:512.
156. Chen J, Dong R, Ge J, et al. Biocompatible, biodegradable, and electroactive polyurethane-urea elastomers with tunable hydrophilicity for skeletal muscle tissue engineering. *ACS Appl Mater Interfaces* 2015;7:28273–28285.
157. Xu C, Yopez G, Wei Z, et al. Synthesis and characterization of conductive, biodegradable, elastomeric polyurethanes for biomedical applications. *J Biomed Mater Res A* 2016;104:2305–2314.
158. Berti FV, Srisuk P, da Silva LP, et al. Synthesis and characterization of electroactive gellan gum spongy-like hydrogels for skeletal muscle tissue engineering applications. *Tissue Eng A* 2017;23:968–979.
159. Guo B, Qu J, Zhao X, et al. Degradable conductive self-healing hydrogels based on dextran-graft-tetraaniline and N-carboxyethyl chitosan as injectable carriers for myoblast cell therapy and muscle regeneration. *Acta Biomater* 2019;84:180–193.
160. Sun Z, Yang L, Zhao J, et al. Natural cellulose-full-hydrogels bioinspired electroactive artificial muscles: Highly conductive ionic transportation channels and ultrafast electromechanical response. *J Electrochem Soc* 2020;167:047515.
161. Seyedmahmoud R, Çelebi-Saltik B, Barros N, et al. Three-dimensional bioprinting of functional skeletal muscle tissue using gelatin methacryloyl–alginate bioinks. *Micromachines* 2019;10:679.

162. Guo B, Glavas L, Albertsson A-C. Biodegradable and electrically conducting polymers for biomedical applications. *Progr Polym Sci* 2013;38:1263–1286.
163. Ross CL, Zhou Y, McCall CE, et al. The use of pulsed electromagnetic field to modulate inflammation and improve tissue regeneration: A review. *Bioelectricity* 2019; 1:247–259.
164. Smith GB. In *Green Nanotechnology, Nanostructured Thin Films IV*, 2011. International Society for Optics and Photonics. San Diego, CA: 2011: 810402.
165. Cruz DM, Tien-Street W, Zhang B, et al. Citric juice-mediated synthesis of tellurium nanoparticles with antimicrobial and anticancer properties. *Green Chem* 2019; 21:1982–1998.
166. Lomelí-Marroquín D, Cruz DM, Nieto-Argüello A, et al. Starch-mediated synthesis of mono-and bimetallic silver/gold nanoparticles as antimicrobial and anticancer agents. *Int J Nanomedicine* 2019;14:2171.
167. Cruz DM, Mostafavi E, Crua AV, et al. Green nanotechnology-based zinc oxide (ZnO) nanomaterials for biomedical applications: A review. *J Phys Mater* 2020;3: 034005.
168. Lu Y, Ozcan S. Green nanomaterials: On track for a sustainable future. *Nano Today* 2015;10:417–420.
169. Medina-Cruz D, González MU, Tien-Street W, et al. Synergic antibacterial coatings combining titanium nanocolumns and tellurium nanorods. *Nanomed Nanotechnol Biol Med* 2019;17:36–46.

Address correspondence to:

Thomas J. Webster, PhD
Department of Chemical Engineering
Northeastern University
216 Cullinane
Boston, MA 02115
USA

E-mail: th.webster@neu.edu

Ebrahim Mostafavi, PhD
Department of Chemical Engineering
Northeastern University
264 Egan Research Center
Boston, MA 02115
USA

E-mail: e.mostafavi@northeastern.edu